THE CANADIAN OPERATIONAL DAILY OBSERVATION AND FORECASTING PROGRAM FOR TOTAL OZONE AND UV INDEX

by
Marcel Vallée
David I. Wardle
Laurence J. Wilson
William R. Burrows
Jim B. Kerr
David W. Tarasick

CARD Research Report No.
(MSRB/ARQX) 94-007

September, 1994

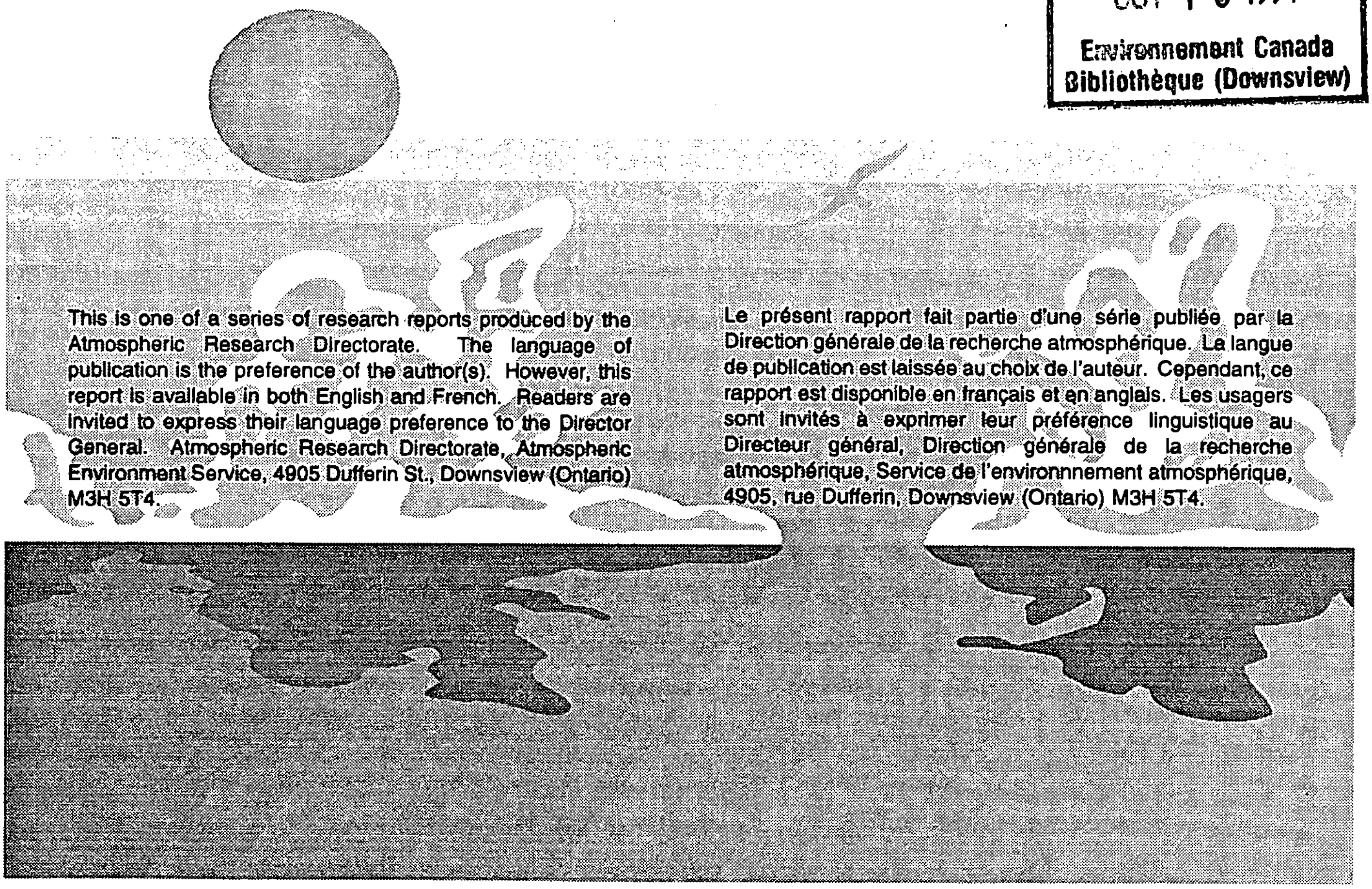

This is one of a series of research reports produced by the Atmospheric Research Directorate. The language of publication is the preference of the author(s). However, this report is available in both English and French. Readers are invited to express their language preference to the Director General, Atmospheric Research Directorate, Atmospheric Environment Service, 4905 Dufferin St., Downsview (Ontario) M3H 5T4.

Le présent rapport fait partie d'une série publiée par la Direction générale de la recherche atmosphérique. La langue de publication est laissée au choix de l'auteur. Cependant, ce rapport est disponible en français et en anglais. Les usagers sont invités à exprimer leur préférence linguistique au Directeur général, Direction générale de la recherche atmosphérique, Service de l'environnement atmosphérique, 4905, rue Dufferin, Downsview (Ontario) M3H 5T4.

RECHERCHE ATMOSPHÉRIQUE

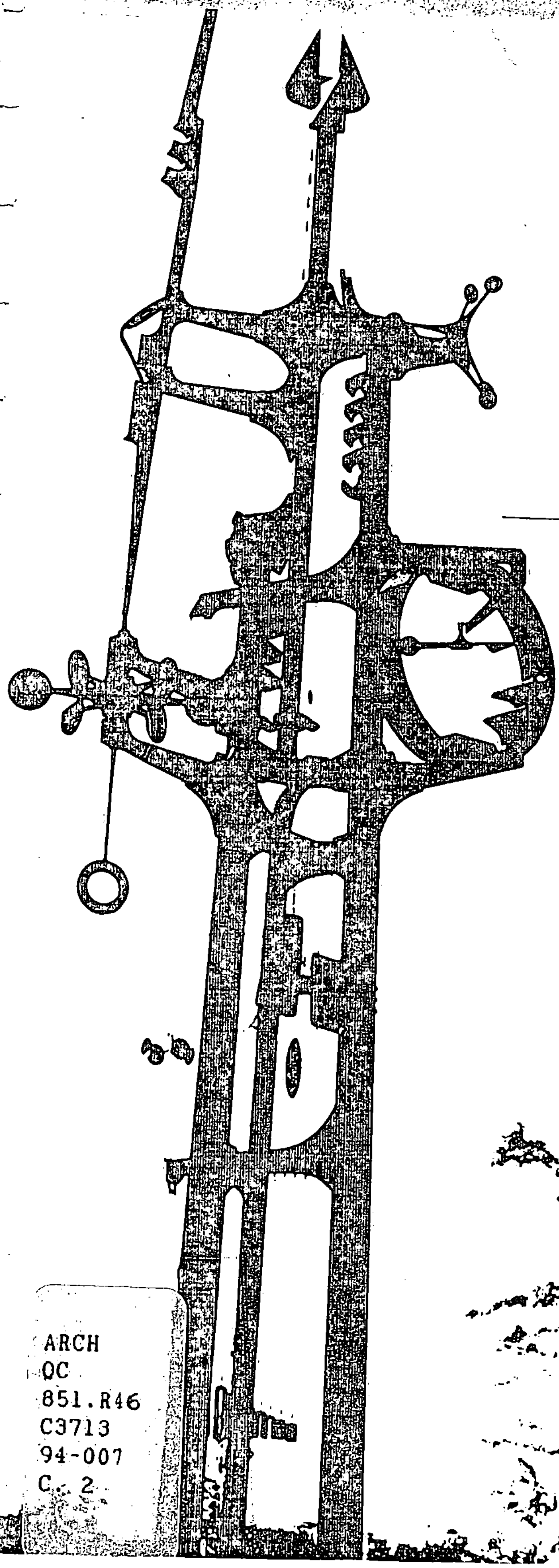

Environment Canada | Environnement Canada

Atmospheric Environment Service | Service de l'environnement atmosphérique

Abstract

This report gives a comprehensive description of the total ozone and UV forecast technique that was implemented and used to produce the UV index forecasts for the summer of 1993. The report also contains a discussion of the various types of total ozone observations that were used in the development and testing of the technique. Test results are shown to support the conclusion that the 1993 technique is considerably better than the 1992 technique and to document the performance of the technique during the summer of 1993.

Ce rapport fait la description de la technique employée pour prévoir l'ozone total et l'indice UV qui a été mis en mode opérationel à l'été 1993. Il comporte également une discussion sur les différentes méthodes d'observation de l'ozone qui ont servi à développer et tester cette nouvelle technique. Une évaluation a été effectuée sur celle-ci qui conclut que cette nouvelle technique est considérablement meilleure que la technique employée en 1992. Les résultats pour l'été 1993 de cette nouvelle méthode de prévision sont également inclus dans ce document.

Contents

Symbols

BIAS	Bias
$CFIELD_{ij}$	(i,j) grid Correction FIELD
CMC	Canadian Meteorological Centre
cov	COVariance
D	Distance
$DCFIELD_{ij}$	(i,j) grid Delta Correction FIELD
DI_{ij}	(i,j) grid ozone initial forecast
DU	Dobson Units
DU_{ij}	(i,j) grid ozone final forecast
F	UV-B flux at surface
FCST	ForeCaST
INDW	INDex of distance Weighting
MAE	Mean Absolute Error
NMC	National Meteorological Centre (U.S.)
OBS	ozone OBServation
PC	Pourcentage Correct
R	residual
R	Earth-Sun distance
R_0	Mean Earth-Sun distance
r	lag correlation coefficient
ρ	lag correlation function
RMSE	Root Mean Square Error
RMSD	Root Mean Square Difference
RV	Reduction of the Variance
S	standard deviation of measurements
SDEV	sample standart deviation
Θ	Zenight angle
TOMS	Total Ozone Mapping Spectrometer
TOVS	Tiros Operational Vertical Sounder
u	airmass
UV	Ultra-Violet
UTC	Universal Time Clock
$\omega_{mem}, \omega_n, \omega_{ij}$	Weighting factors
$\omega_{tmp}, \omega_{spc}$	Weighting factors
$\boldsymbol{x}$	ozone amount/1000
X	independant variable
XINFL	distance X of INFLuence
XMEM	distance X of MEMory

Aknowledgements

We wish to thank C. Paterson of the Meteorological Research Branch for his technical support to the daily data archives and the technique development. We are grateful to D. Soucy, M. Jean, R. Verret and G. Desautels of the Canadian Meteorological Center, for their sgnificant contribution in implementation of the daily total ozone and UV index forecast in operational mode. We wish to thank P. Guimaraes, R. McPeters, A. Krueger, members of the TOMS Nimbus Experiment and Ozone Processing Teams, and the National Space Science Data Center, for supplying the CD-ROM copy of the TOMS data set. Also thank to S. Lambert for providing the meteorological data, obtained from the National Center for Atmospheric Research in the United States.

References

Brewer, A. W., 1949: Evidence for a world circulation provided by the measurements of helium and water vapour distribution in the stratosphere. Quart. J. Roy. Meteorol. Soc., 75, 351-363.

Brockwell and Davis, 1991: Time Series; Theory and Methods, Second Edition, 557pp.

Burrows W.R., Vallée M., Wardle D.I., Kerr J.B., Wilson L.J, and Tarasick D, 1994: The Canadian operational procedure for forecasting total ozone and UV raridation. Accepted by the Royal Meteorological Society, Meteorological Applications, 48pp.

Burrows W.R., Vallée M., and Wilson L.J., 1992: Climatology of daily total ozone and ultraviolet-B radiation levels, Environment Canada Research Report MSRB 92-005, 204pp.

Burrows W.R., Wilson L.J., and Vallée M., 1993: A statistical forecast procedure for daily total ozone based on TOMS data, Preprints 13th Conference on Weather Analysis and Forecasting, 1-6 August 1993, Vienna, VA, Amer. metor. Soc., in Press.

Chesters, D. and Neuendorfer, A., 1991: Comparison between TOMS, TOVS, and Dobson observations, satellite and surface views of total column ozone. Global and Planetary Change, 4, 61-67.

Danielson E.F., 1968: Stratospheric-tropospheric exchange based on radioactivity, ozone, and potential vorticity. J. Atmos. Sci., 25, 502-518.

Dobson, G.M.B., Brewer A.W., and Cwilong B.M., 1946: Meteorology of the lower stratosphere. Proc. R, Soc. London, A185, 144-175.

Dutton, J. A., 1976: "The Ceaseless Wind an introduction to the theory of atmospheric motion". McGraw-Hill, New York. ISBN 0-07-018407-0. pp. 92-94.

Evans W.F.J., Fast H., Forester A.J., Henderson G.S., Kerr J.B., Vupputuri R.K.R.,Wardle D.I., 1987: Stratospheric Ozone Science in Canada. Environment Canada Research Report ARD 87-3, 127pp.

Gowan, E.H., 1931: Effect of ozone on the temperature of the upper air. Monthly Weather Review, 59, 80-81.

Holton J.R., 1979: An Introduction To Dynamic Meteorology, Second Edition, Academic Press, New York, N.Y., pp317-321.

Johnson J.C., 1954: Physical Meteorology, M.I.T. Press Cambridge, Mass., 339-353.

Naujokat B., et al., 1992: The Stratospheric Winter of 1991/92. The winter of the European Arctic Stratospheric Ozone Experiment, Beilage Zur Berliner Wetterkarte, 68/92, 5018/92.

Planet, W.G., D.S Crosby, J.H. Lienesch and M.L. Hill, Determination of total ozone amount from TIROS radiance measurements, J. Climate. Appl. Meteor., 23, 308-316, 1984.

Riishojgaard L.P., Lefèvre F., Cariolle D., and Simon P., 1992: A GCM simulation of the northern hemisphere ozone field in early February 1990, using satellite total ozone for model initialisation. Ann. Geophysicae, 10, 54-74.

Schubert S,D., and Munteanu M.J., 1988: An analysis of tropopause pressure and total ozone correlations. Mon Weather Rev., 116, 569-582.

Vaughn G. and Price J.D., 1991: On the relation between total ozone and meteorology. Q. J. Royal Meteorol. Soc., 117, 1281-1298.

Wilson L.J., Vallée M., Tarasick D., Kerr J.B., and Wardle D.I., 1992: Operational forecasting of daily total ozone and ultraviolet-B radiation levels for Canada, Environment Canada Research Report MSRB/ARQX 92-004, 29pp.

Introduction

On June 9, 1993, a new total ozone thickness and UV forecast technique was launched at the Canadian Meteorological Centre (CMC) in Montreal. This new implementation is described in Burrows et al, (1993) and has been shown in verification tests to be a considerable improvement on the previous ozone and UV technique (Wilson et al., 1992). The new technique follows a perfect prog statistical formulation and consists of a set of six regression equations for three different latitude bands of the northern hemisphere and for two seasons. Forecasts using the equations are produced for the entire northern hemisphere by linearly blending the output of the equations for the different latitude bands. Seasonal blending is also done to ensure smooth transition between the summer and winter seasons.

The equations were developed using forward stepwise regression. Predictor values were obtained from analyses of upper tropospheric and lower stratospheric meteorological variables while the predictand consists of gridded observations of total ozone (in Dobson units) from the Total Ozone Mapping Spectrophotometer (TOMS) aboard the NIMBUS-7 satellite. The development sample size was 5 years, 1987 to 1991.

The equation development resulted in selection of 5 to 8 predictors for each latitude band and each season. One of the most important predictors selected was ozone climatology, computed from the TOMS data (Burrows et al., 1992). Others selected include air temperatures, heights and vorticity at high troposphere and lower stratospheric levels, and occasionally, coriolis parameter and latitude.

In operations, total ozone and UV forecasts are prepared twice daily and year round. The operational procedure is in three parts: First, the equations are run using forecast values of the predictors from the operational global spectral model. Forecast projections are 18 hours and 42 hours for the 00:00 UTC run and 30 hours for the 12:00 UTC run. These times are chosen to give forecasts valid near local solar noon. Second, the output from the equations is subjected to a correction procedure which uses observations from the Canadian network of Brewer Spectrophotometers. Third, the corrected forecasts of total ozone are run through an empirical formula to generate the UV forecasts. Both the ozone and the UV forecasts are formatted at CMC into bulletins and charts for output to users in regional forecast offices.

The performance of the previous and new technique have been compared for the summer of 1992, using observations from the Brewer network, to determine the magnitude of improvements that were realized by the new technique. Also, a comprehensive verification of the new technique has been carried out for the summer of 1993.

This report presents first a comprehensive discussion of the sources of total ozone observations, including a direct comparison of these data for a period in the fall of 1991. This is followed by a summary of the climatology of ozone, and a description of its relationship with UV radiation at the ground. Then, in chapter 2, the forecast technique is described along with the correction procedure. Finally, chapter 3 is devoted to a discussion of the evaluation of the forecasts, both with respect to the previous (1992) system and for the summer of 1993. A case study is also included.

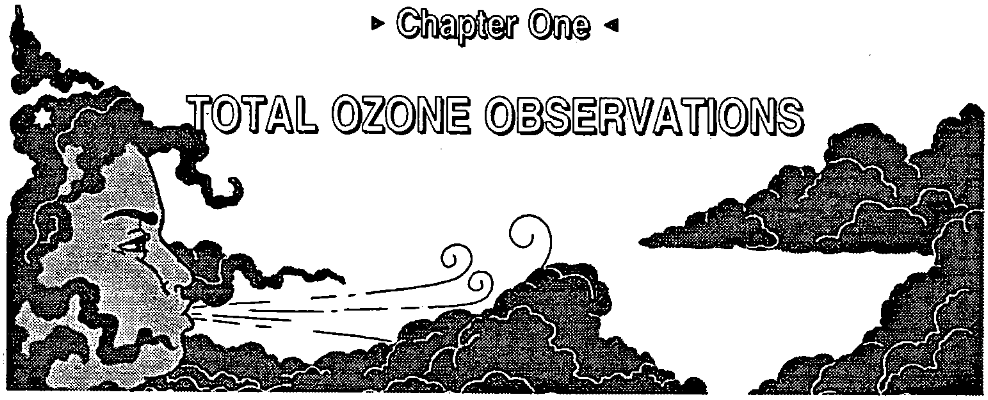

1.1 Comparison among Brewer, TOMS and TOVS total ozone measurements

This section describes direct comparison experiments among Brewer, TOMS, and TOVS (Tiros Operational Vertical Sounder) measurements of total ozone. The latter two instruments are aboard polar orbiting satellites and give global or near-global data coverage. Brewer data is available only for Canadian stations for this comparison. The Brewer spectrophotometer is shown in figure 1.1)

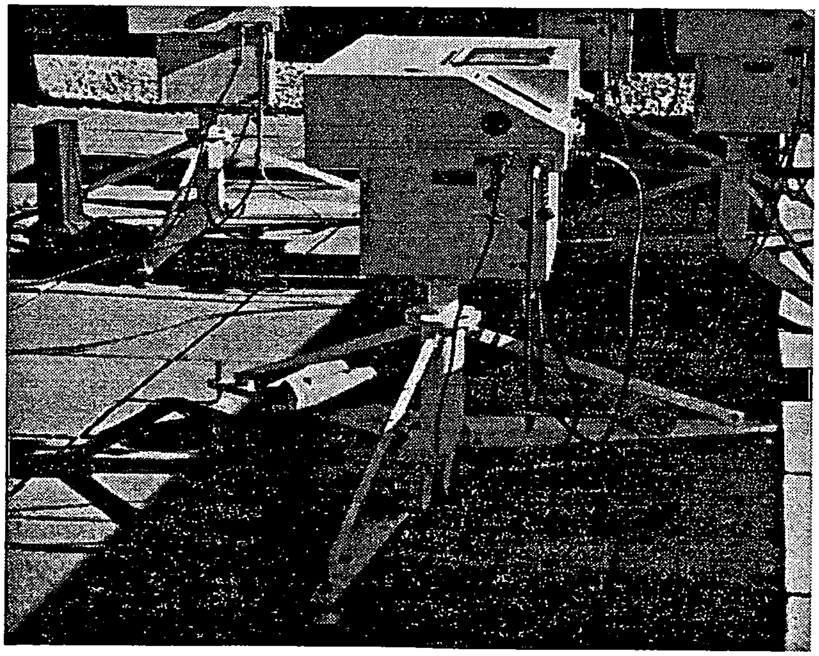

Figure 1.1: The brewer spectrophotometer instrument.

The TOMS instrument measures ozone by sensing the differential scattering of sunlight in two different radiation bands. Ozone is determined by the ratio of returns from the 312 nm and 331 nm bands. Ozone strongly absorbs radiation in the 312 nm band, but only weakly in the 331 nm band. The resolution is about 40km square. TOMS data are archived at NASA Goddard Space Centre, and are made available to users in gridded form with a mesh size of 1.25 degrees longitude by 1 degree latitude. There is no data for dark areas of the earth. The orbit of the satellite ensures that data are valid for approximately local solar noon, and each day's data is archived as one gridded dataset.

TOVS total ozone is inferred using a statistical relationship for which the input is radiances of the infrared channels 9.71, 11.11, 14.95, 14.71 and 14.49 μm and the short wave channel 5180 μm, all expressed as brightness temperatures. The satellite data is related statistically to measurements of total ozone from the Dobson spectrophotometer, under clear skies. Several regression equations have been derived, for different seasons and latitude bands. When the sky is partly cloudy, clear sky radiances are estimated using a function called TARM (Tiros Atmospheric Radiance Module) for input to the regression equations. Data is not available when it is cloudy. TOVS data are archived in the form of 65 by 65 polar stereographic grids covering the northern hemisphere, with a resolution of 381 km true at 60 north. During interpolation to the grid, missing values are filled in. It is this gridded form of the data that was used in the comparison test.

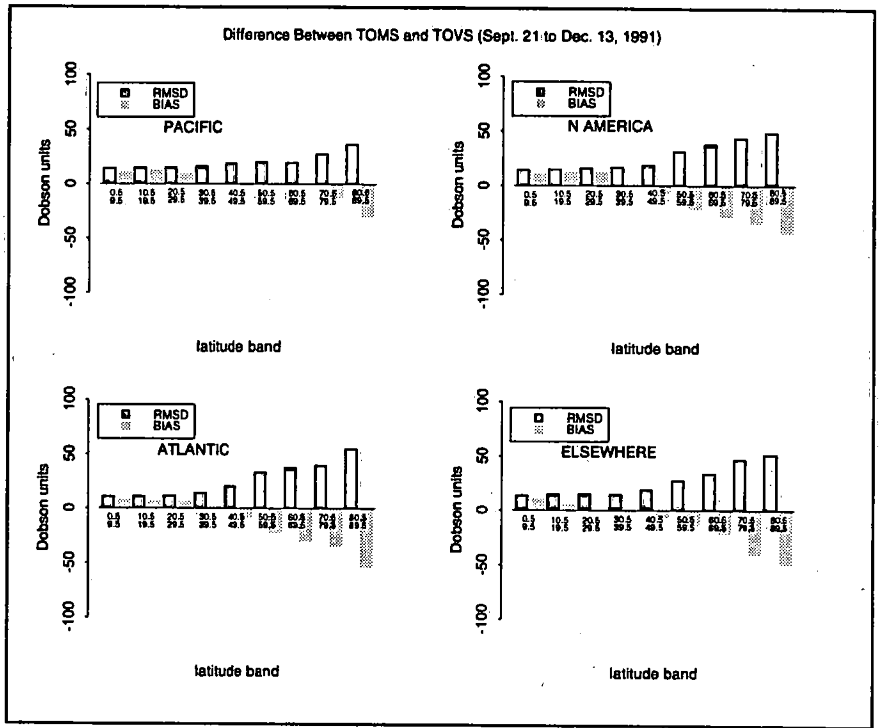

Figure 1.2: Statistical result between TOMS and TOVS within different areas over northern hemisphere.

The test period was September 21 to December 13, 1991, the period for which TOVS data is available. Two types of comparison were carried out: First, the two types of satellite data were compared, and second, each satellite dataset was compared with the available Brewer observations for the test period. For the first test, the TOVS data was interpolated by cubic spline to the latitude-longitude grid of the TOMS data. The northern hemisphere was divided into four different regions based on longitude, and 9 latitude bands, for a total of 36 separate regions for calculation of difference statistics. The longitudes are: Atlantic: Greater than 10.0 degrees west to 60.0 degrees west; North America: Greater than 60.00 degrees west to 130.0 degrees west; Pacific: Greater than 130.0 degrees west to 180 degrees; and Elsewhere: less than 180.0 degrees east to 10.0 degrees west. Latitudes are divided into bands of 10 degrees from 0 degrees to 90 degrees. The reason for the longitudinal categorization is to see if any systematic differences show in the statistics between land areas and ocean areas.

Figure 1.2 shows the results of the TOMS-TOVS comparison. It can be seen that the mean difference at all longitudes tends to be positive near the equator (TOMS higher than TOVS) and negative toward the poles (TOVS higher than TOMS). This is consistent with Chesters and Neuendorfer, 1991, who stated that TOVS may underestimate total ozone near the equator due to cirrus clouds, and that TOMS estimates of total ozone are much lower than TOVS estimates near the edge of polar night.

Root mean square differences are lowest near the equator at all longitudes (of the order of 10 DU), and rise noticeably north of 50 degrees north. It is known from earlier studies (e.g. Riishojgaard et al, 1991) that TOMS observations show higher error levels for sun angles lower than 20 degrees. To check this further, figure 1.3 shows RMS differences between TOMS and TOVS for all longitudes as a function of zenith angle. The RMSD rises steeply from about 15 DU for zenith angles of 60 degrees to about 40 DU for zenith angles of 85 degrees. TOVS accuracy would not be expected to vary significantly with zenith angle since the source data is (mainly) infrared radiances from the earth.

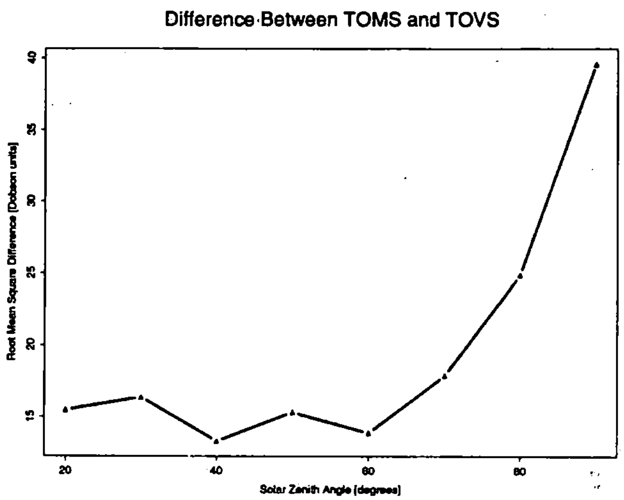

Figure 1.3: Difference between TOMS and TOVS in relation with the sun angle.

Since the accuracy of the TOVS data depends to some extent on the accuracy and representativeness of the surface temperatures that are used to estimate brightness temperatures for the regression equations, it was expected that there might be some variation in the RMS differences with longitude, depending on whether observations were taken over land or sea. Figure 1.2 does not indicate any significant differences in either the bias or the RMS difference between land and sea observations. One possible explanation is that errors in surface temperature retrievals are also reflected in retrievals in the other channels, and tend to cancel out.

For the second comparison, both TOVS and TOMS datasets were interpolated to the locations of Brewer spectrophotometer. A total of 157 observations are available for the test period, thus there are 157 matches between the Brewer data and each of the satellite datasets. Results of this comparison are shown in figure 1.4 in the form of two histograms giving frequencies of differences in categories of 10 Dobson units. Mean difference (bias), mean absolute difference and root mean square difference statistics are also shown. Results indicate that the Brewer observations are higher than the TOMS observations on average by 2 to 3%, but that the Brewer observations are within 1% of the TOVS observations on average. Root mean square differences, however are slightly higher for the TOVS data than for TOMS data.

The overall bias in the TOMS data can be attributed to the previously-noted tendency to underestimate ozone amounts near the polar night. To check this, we eliminated from the sample all cases with a solar zenith angle greater than 70 degrees, which reduced the sample size to 103 cases. Histograms

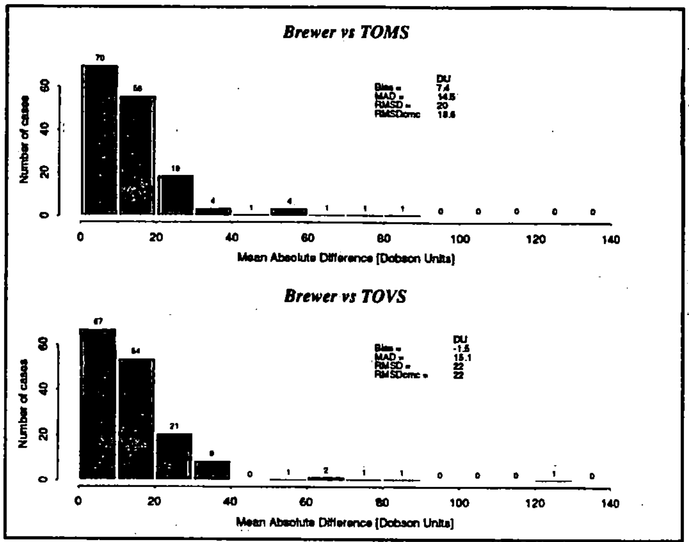

Figure 1.4: Histogram comparing different intruments of total ozone measurement.

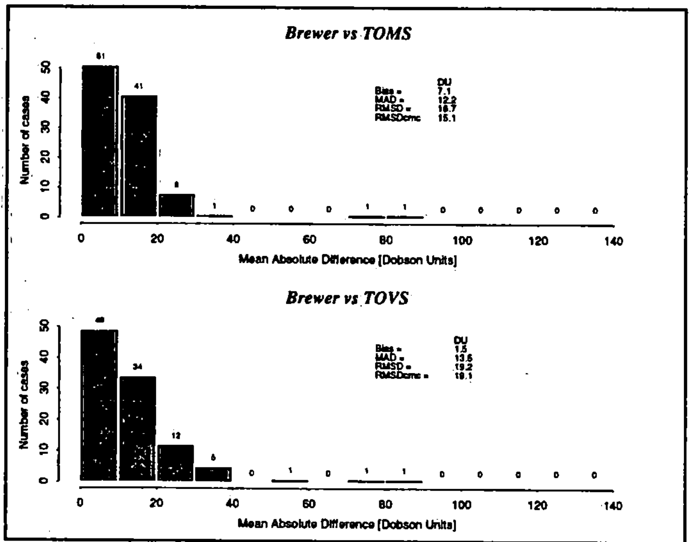

Figure 1.5: Same has 1.4 but with a solar zenith angle greater than 70 degrees.

for the reduced sample are shown in figure 1.5. The mean difference between TOMS data and Brewer data didn't change very much, but the RMS difference was lowered by 4 DU for the TOMS data. However, the RMSD for the TOVS data also decreased by about the same amount. Closer examination of both figures reveals that there is a tendency for the extreme differences to be eliminated when high solar zenith angle cases are removed. Since both the Brewer and TOMS instruments are solar instruments, perhaps all that can be concluded is that solar based measurements are less reliable near the edge of polar night. In particular, the one very large difference of over 120 DU between TOVS and the Brewer observation is more likely to be due to an error in the Brewer observation than in the TOVS data.

1.2 Total Ozone Climatology

The climatology of total ozone is characterized by very large latitudinal and seasonal variations. Details of the climatological distribution of ozone are given in Wilson et al., 1992, and will not be reproduced here. The mean distribution is thought to be maintained by planetary scale transport processes in the upper troposphere and lower stratosphere. Since individual ozone molecules have very long lifetimes (of the order of months) in these regions, it is possible for them to be transported over very long distances by planetary scale motions.

The main source region for ozone is in the tropical stratosphere above 25 km, where oxygen atoms are photodissociated by ultraviolet radiation (Holton, 1979). The ozone is then transported away from the tropics by the Hadley circulation (Brewer, 1949), and downward towards the poles. The observed maximum is at about 60 degrees north (and south) latitude, occurring in the early spring. This can be explained by considering that the transport mechanisms are most active in winter when the average circulation is strongest, and by also considering that destruction of ozone by solar processes is weakest in winter. Ozone gradually builds up in the northern hemisphere through the winter, then in summer, destruction is more active, the circulation is weaker and so losses exceed the transport into midlatitudes, causing the ozone to slowly deplete through the summer months, reaching a minimum in October. The amplitude of the annual cycle is greatest also near 60 degrees north. At southern Canadian latitudes, the annual cycle has a peak to trough difference of about 100 Dobson units, almost 1/3 of the annual average. In the tropics the annual cycle has an amplitude of only about 20 DU.

Since the climatological variations are maintained by large scale processes, they cannot be described accurately by a short range forecast system based on synoptic modelling. The climatological signal must be added, and that is why climatological information is used in the statistical forecasting technique described below.

The TOMS data has been used to produce a climatological atlas of total ozone for the Northern Hemisphere. The atlas is published as a Research Directorate internal report (Burrows et al., 1992). The weekly climatology used for that atlas has been further processed for use in the statistical forecast technique development. The weekly mean maps were filtered with a 9 point triangle smoother. Thus each climatological value is a weighted mean of the current weekly average ozone value and values for up to four weeks before and four weeks after the current week. Figures 1.6 and 1.7 show the effect of the smoother. Because the original weekly values are already averaged over 13 years and over one week, the characteristics of the field do not change greatly. Following application of the triangle smoother, a daily climatological value is interpolated using Akima cubic spline. Figure 1.8 shows the original weekly average values for Toronto, along with the daily interpolated values after processing.

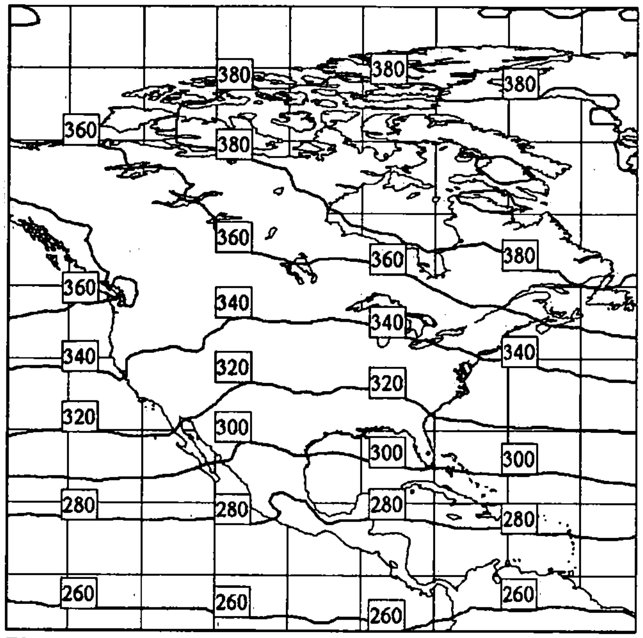

Figure 1.6: Weekly climatology from TOMS data, from May 28 to June 3. Values are in Dubson units.

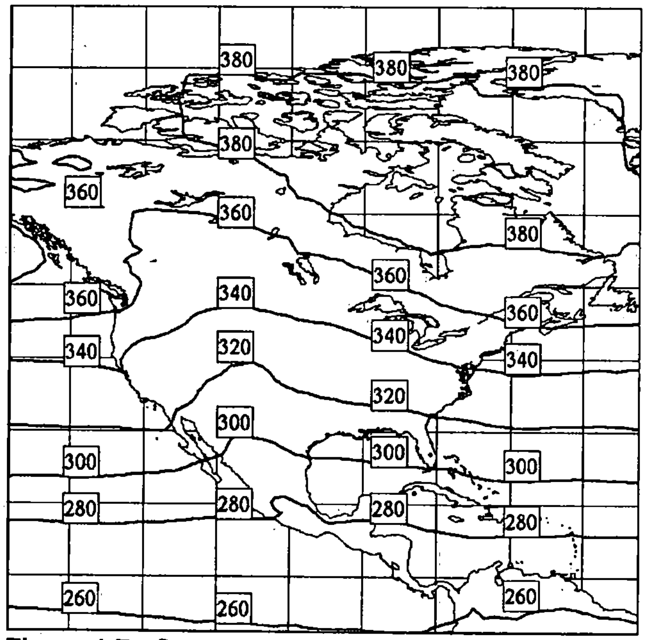

Figure 1.7: Ozone climatology for june 1. Values are in Dobson units.

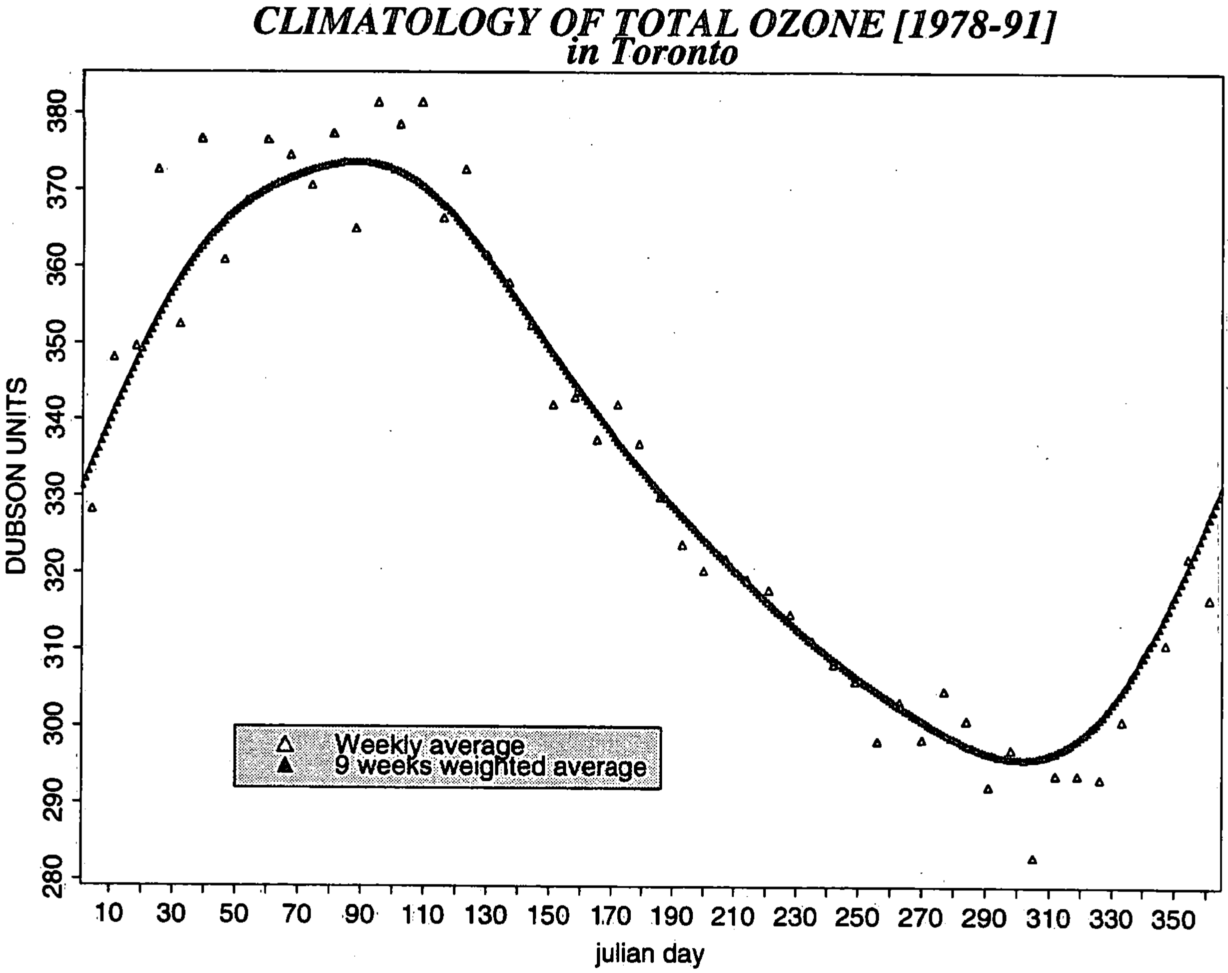

Figure 1.8: Ozone climatology in Toronto. The white triangles are the weekly mean and the black triangles are the daily mean.

For the forecast technique, we needed a complete climatology for all latitudes and all seasons, which meant that it was necessary to fill in for the missing TOMS data over polar night areas. This was done as follows: For latitude 51.5N, where reasonably accurate data are available for the whole year, a set of 240 spline functions was built for the annual cycle, one for each longitude. Then, for each week where data are missing, a value was estimated. The estimated value consists of the value extracted from the spline function for the appropriate week and longitude, plus the difference between the observed value at 51.5N and the observed value at the appropriate latitude for the first week when all data is available (week 12 at the end of March). This method assumes that the shape and phase of the annual cycle is preserved northward of 51.5 N (probably not a bad assumption) and that the north-south differences in climatological values for week 12 are preserved for weeks 1 to 11. The same process of estimation is used in the early winter, with week 38 for the horizontal differences and latitude 51.5 N for computation of the spline. It is tempting to make greater use of the observations adjacent in space and time to the edge of polar night, but the TOMS data is known to be somewhat unreliable near the edge of polar night.

1.3 The observation bulletin

SXCN10 bulletins are messages that summarize current day measurements of ozone and UV radiation made by Brewer spectrophotometers (figure 1.1). They are put on the Environment Canada Wide Area Net(WAN) by the local computers that operate the Brewers at the 13 sites (Saturna, Edmonton, Saskatoon, Regina, Winnipeg, Churchill, Toronto, Montreal, Halifax, Goose Bay, Resolute Bay, Eureka and Alert) in the Canadian ozone network as shown in figure 1.9 and table 1.1. A new bulletin is generally transmitted after each successful measurement of ozone and it will include all the information of previous bulletins on that day from the same station plus whatever new measurements are available. SXCN10 bulletins can be accessed in the same ways as all the other weather bulletins.

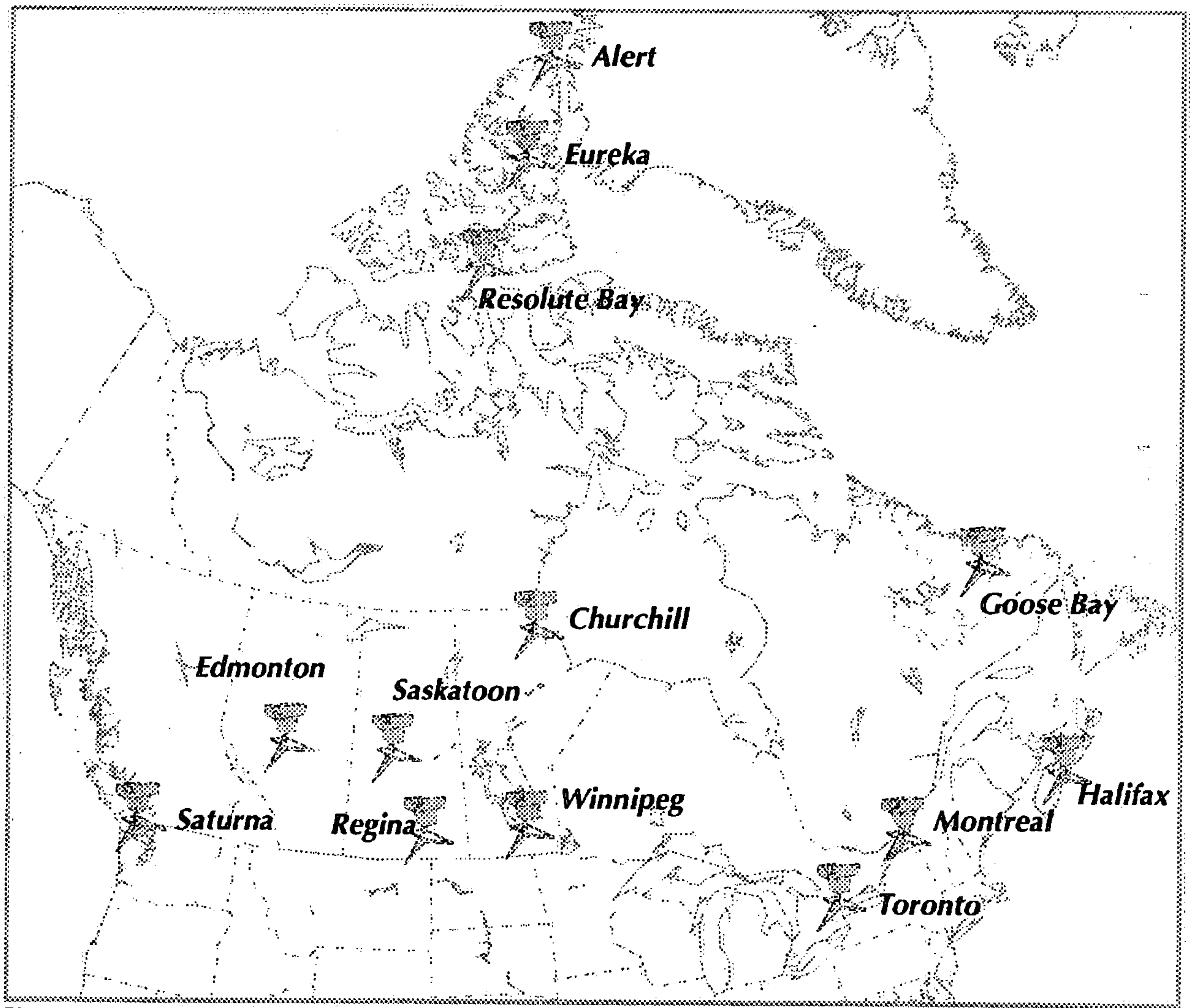

Figure 1.9: Location of the canadian brewer instrument.

The SXCN10 bulletin is an abbreviated form of the daily summary of Brewer measurements that is generated on site just prior to midnight (local time). The daily summary includes information on other types of measurements and several diagnostic tests that the Brewer performs throughout the day. It may be several pages long. However, this is a very small fraction of the 200Kbytes of raw data that a single Brewer records each day. The raw data is not accessible via the WAN but it is archived in Toronto on the Brewer Data Management System.

Table 1.1: Location and data record lenght operational of the brewer *instruments.*

Station:	Lat	Lon	Since
Edmonton (YXD)	53.6N	114.5W	1983
Toronto (YYZ)	43.8N	79.5W	1983
Saskatoon (YXE)	52.1N	106.7W	1984
Goose Bay (YYR)	53.3N	60.3W	1985
Churchill (YYQ)	58.8N	94.1W	1986
Resolute Bay (YRB)	74.7N	95.0W	1987
Alert (WLT)	82.5N	62.3W	1988
Saturna (SAT)	48.8N	123.1W	1988
Bedford (WHZ)	44.7N	63.7W	1992
Winnipeg (YWG)	49.9N	97.2W	1992
Montreal (YUL)	45.5N	73.8W	1993
Eureka (WEU)	50.7N	104.4W	1993
Regina (WQR)	50.2N	104.7W	1994

A typical SXCN10 bulletin is shown in Table 1.2. It contains some site information in the header, a block of ozone measurements including means and standard deviations and, finally, a block of UV measurements.

The header, in its first line, states the site location and the serial number of the Brewer there. In the second line the words "preliminary data" are important; the near real time data in the bulletin may need to be changed slightly for various reasons. The "Local Date" is given to help avoid the confusion that can arise particularly at the western Canadian stations where afternoon measurements occur when Greenwich time has already advanced to the next day. The four numbers on the last line of the header are used in the algorithm that converts raw Brewer signals into ozone and sulphur dioxide values. They are used as one form of quality control check on the data.

Each line in the following block describes an ozone and sulphur dioxide "measurement." When configured to measure ozone in the standard technique, the signals from the Brewer comprise a set of five numbers that are each proportional to the strength of radiation at five different wavelengths averaged over a period of about 30 seconds. These numbers with the appropriate algorithm yield an ozone value and an SO_2 value. In the course of the "measurement" , which takes about three minutes, five such sets of such numbers are acquired and five values for ozone and SO_2 are computed from them.

The meaning of the entries in each ozone measurement line is as follows:

Type: DS and FM, which signify "Direct Sun" or "Focused Moon," are the only measurement types transmitted in SXCN10. In these types, the Brewer measures only the radiation that comes from the direction of the sun or moon, not from other parts of the sky. The "0", "1" or "2" after

"DS" indicates what, if any, optical attenuator is inserted in the beam at the front end of the Brewer. If the sunlight is intense, the strongest attenuator, which is "2", is normally in place.

Table 1.2: The SXCN10 bulletin.

SXCN10 CWSE 290429

STONY PLAIN OZONE - BREWER # 013
PRELIMINARY DATA - LOCAL DATE JUN 28/93
LATITUDE - 53.55 : LONGITUDE - 114.5
ETC'S - O3/SO2 - 3048 / 3331 : ABSORPTION - .343268 / 1.137718

TYPE	TIME-GMT	TEMP	AIRMASS	OZONE	ERROR	SO2	ERROR
DS 0	14:10:44	18	2.530	311.1	+0.4	0.5	+0.3
DS 0	14:18:09	18	2.426	310.5	+2.0	0.2	+0.6

DAILY MEANS 18 2.477 310.8 0.4
STANDARD DEVIATION +0.4 0.2

SUMMARY OF BREWER UVB SCAN MEASUREMENTS FOR JUN 28/93

TIME?GMT?	TEMP	ZENITH ANGLE	AIRMASS	UV INDEX
12:50:41	16	78.63	4.691	0.2
14:03:15	17	68.36	2.654	0.8
14:44:55	19	62.21	2.119	1.4
15:09:58	20	58.49	1.896	1.4
15:51:52	21	52.33	1.627	1.7
16:33:56	22	46.36	1.444	1.7
17:16:16	23	40.80	1.318	1.8
17:31:04	23	39.02	1.284	1.3
18:12:59	23	34.64	1.213	2.5
18:56:01	24	31.55	1.172	2.3
19:39:05	24	30.36	1.158	2.0
19:46:57	24	30.37	1.158	2.7
20:35:07	23	32.00	1.178	2.1
21:19:56	23	35.58	1.227	2.4
22:03:35	24	40.42	1.310	2.2
22:47:26	24	46.15	1.438	1.2
23:31:27	24	52.39	1.629	1.7
00:18:46	26	59.35	1.942	1.7
01:08:43	26	66.75	2.487	0.7
02:14:23	25	76.18	3.966	0.2

GMT: The Greenwich Mean Time at the middle of the observation.

TEMP: The internal instrument temperature (actually the temperature of the photomultiplier).

AIRMASS: The relative path length of the sunlight through the ozone compared with the path length if the sun were at zenith (i.e. vertically overhead). The angle between the sun and the vertical is called the ZENITH ANGLE. The airmass is approximately equal to the secant of the zenith angle, except when the sun is near the horizon.

OZONE The average of the five ozone values derived from each of the five 30-second periods.

ERROR: The standard error about the above mean.

SO2: As above for sulphur dioxide.

ERROR: As above for sulphur dioxide.

When measuring the UV-B, the Canadian network Brewers, and most others in the world, are currently programmed to measure at seventy one wavelength settings. This is done by scanning with an increment of 0.5 nm from 290nm up to 325nm and back down to 290nm. The double scan takes about seven minutes. The radiation that is measured is the Downward Horizontal Spectral Irradiance also known as the Spectral Global Radiation (i.e. what falls on a horizontal surface from all directions in the sky, including from the sun).

The UV index, which is listed in SXCN10, is the quantity for which Environment Canada issues daily forecasts. The measured value here is derived by multiplying each of the 71 measurements in the uv scan by the factor determined from the McKinley-Diffey erythemal action spectrum, adding the products and dividing by $25Wm^{-2}$. The very small contribution from radiation between 325nm and 400nm, which the Brewer does not measure, is estimated from the measurement at 324nm.

The contents of the SXCN10 bulletin may be changed in future just as new types of measurements will be included in the schedules of the network Brewers. The above description applies in the SXCN10 format used throughout 1993.

1.4 Computing the UV index from ozone

The computation is done from an empirical relation derived from clear sky measurements made at Toronto during 1990 -1991. Clear sky in this context means substantially free from clouds. The dataset therefore includes the effects of whatever particulate were present, and the relationship can be expected to estimate typical cloud free values encountered in Toronto which should be less than for cloud free days with especially clean air.

The following equaion was fitted to the data by choosing the five parameters a..e so as to minimise the squared deviations in UV-B:

where F = UV-B flux at surface (mWm^{-2})

$$F = \frac{R_0^2 \cos\theta}{R^2} \exp[a + b(ux) + c(u) + d(ux)^2 + e(u)^2] \quad (1.1)$$

Θ = zenith angle
u = airmass
x = ozone amount / 1000
R = Earth-Sun distance on given day
R_0 = Mean Earth-Sun distance

The fitted values are: a= 7.178 b= -3.842
c= -0.731 d= 1.574
e= 0.1279

As such the formula fits the measured data with a standard deviation of about 7% which is about the same as the intrinsic variability of the data.

There is some physical significance in the form of the equation. With the parameters "d" and "e" set to zero, it exactly describes the behaviour of the direct beam component of single wavelength radiation.

The $(R_0/R)^2$ term expresses precisely the modulation of the solar energy arriving at the top of the earth's atmosphere due to the varying distance from the sun. The distance varies by about 3% from minimum to maximum and, consequently, the intensity varies by about 6%.

The term exp(a) expresses the top-of-the-atmosphere UV-B radiation with the sun vertically overhead and the earth at its mean distance from the sun.

The term cos(Θ) expresses the diminution of the radiation due to the sunlight arriving at a slant compared with coming vertically downwards. This term together with the distance term exactly expresses the variation of downward irradiance above the atmosphere. It would also correctly express the slant induced variation at the earth's surface if all the radiation were in the direct beam and the sky were dark. In fact, at UV-B wavelengths, similar amounts of radiation come from the sky and the direct beam.

If the formula were applied to single wavelength radiation, the terms "b(ux)" and "c(u)" would describe losses of the direct beam radiation due to ozone absorption and to Rayleigh scattering. The value of "b" would be the ozone absorption coefficient and "c" the Rayleigh scattering coefficient per atmosphere at the wavelength in question.

The equation must also take into account diffuse radiation at many wavelengths and, not surprisingly, the single wavelength direct beam formulation has been found to be inadequate. Adding the squared terms $d(ux)^2$ and $e(u)^2$ yielded a relation that could fit the data to the required accuracy. There is no simple physical interpretation of these terms. Their justification and that of the whole formulation is pragmatic.

Comparison with output from radiative transfer models and a few measurements at extremely low ozone values in 1993, indicate that the empirical relation may slightly underestimate the UV-B when the ozone is less than 280 DU.

Finally, a UV index is then produced by dividing F by $25Wm^{-2}$. An index of 10 corresponds to a typical mid summer day over an equatorial region (i.e. 250 DU). We then divided the UV index into 4 categories. An index less than 4 represents the category LOW, meaning an average of more than one hour before the average type of skin (without any tan) burns. An index of 4 and less than 7 represents the category MODERATE, giving burns in about 30 minutes, an index of 7 and less than 9 represents the category HIGH, giving burns in about 20 minutes and finally an index of 9 or more represents the category EXTREME, giving burns in less than 15 minutes.

▸ Chapter Two ◂

THE OZONE AND UV INDEX FORECAST TECHNIQUE

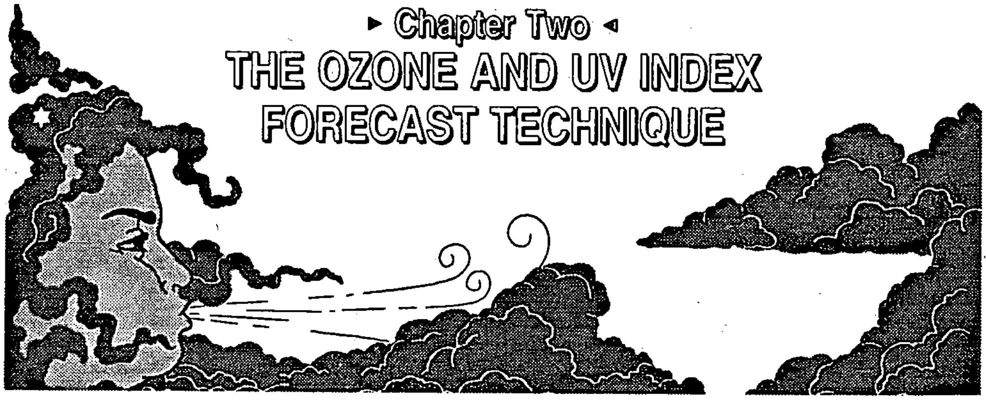

2.1 Predictand, predictors and development dataset

The ozone observations used in development are from the TOMS dataset mentioned above. For equation development, we used only the last 5 years of the data, 1987 to 1991 so that the dependent sample climatology would be as close as possible to the current average levels of total ozone. The TOMS data were interpolated to a 254 km polar stereographic grid (true at 60 N) using bicubic splines, in order to match the predictor dataset that was used in development. The development sample grid area extends from 10 to 180 degrees W and from 10 to 75 degrees N. All observations with a sun angle less than 20 degrees were removed before processing. The observations are assumed to be valid at local noon; each grid map of observations covers one day, which means that a collage of valid times is included in terms of UTC.

Meteorological predictors were chosen on the basis of previous studies on the relationship of total ozone to synoptic meteorological variables. These include Gowan (early 1930s) who showed a correlation between ozone and stratospheric temperature profiles; Dobson et al. (1946) and Johnson (1954) who relate high concentrations of ozone in upper troughs and low concentrations in upper ridges to upper tropospheric convergence and divergence respectively; Danielson (1968) who correlated ozone concentration with potential vorticity; Schubert et al. (1988), who showed a relationship between ozone thickness and tropopause height; Naujokat et al. (1992), who related total ozone to 300 hPa height, and finally, Vaughan and Price (1991), who found a strong relationship with absolute vorticity and isentropic potential vorticity.

The meteorological predictors offered include temperature, geopotential height, wind components, potential vorticity and relative vorticity for several constant pressure levels in the upper troposphere and lower stratosphere. Attempts were made to identify the tropopause level explicitly and use that as a predictor, but it was felt that the analysis resolution (and model resolution) of the tropopause would not be sharp enough for this to be a reliable predictor. Instead, temperature and geopotential height together represent the tropopause. Because of uncertainties in the accuracy of model forecasts above 70 hPa, no predictors were offered for higher levels.

Predictor values come from NMC upper air analyses, on a 254 km polar stereographic grid. The predictor values are matched temporally to the TOMS data by interpolating them (linearly) to local noon.

Non-meteorological predictors include ozone climatology taken from the entire TOMS dataset, along with latitude, longitude and the coriolis parameter. It is considered necessary to include climatological and latitudinal predictors because the strong seasonally- and latitudinally-varying climatological signal in the total ozone, which is determined by large-scale long term transport processes, could not be captured adequately using the synoptic scale meteorological predictors.

The dependent sample was stratified into two seasons, summer (April 15 to September 21) and winter (September 22 to December 31 and January 1 to April 14). The seasons were chosen to separate the winter period, which is characterized by higher day to day variability of ozone from summer, with lower variability and greater importance in the UV index program.

The two seasonal samples were further divided on the basis of latitude. Three latitude belts were identified for each season, based mainly on the climatological distribution of potential temperature as shown in Dutton, 1976, figs. 4.11 and 4.12. The aim is to separate barotropic regions to keep the samples as homogeneous as possible. For summer, the three latitude belts are: 10 to 30 N (tropical), 30 to 50 N (mid-latitude) and 40 to 75 N (polar). In winter, the three latitude belts are: 10 to 23 N, 23 to 43 N and 33 to 75 N. The use of overlapping regions helps ensure spatial consistency in the forecasts across the boundaries. In application of the equations, the polar equations are used for polar night latitudes and the tropical equations are assumed valid down to the equator.

Finally, because of high spatial and temporal correlations in the dataset, the data was "thinned" out by using every third grid point in the regression. We were still left with development sample sizes of between 12,000 cases and 100,000 cases, depending on the season and latitude band.

2.2 Regressions and results from the dependent sample

Forward stepwise regression (with a backward look) was carried out on the development dataset, resulting in a total of six regression equations, for two seasons and three latitude bands. The results of the screening are shown in Table 2.1. It can be seen that the first-chosen predictors tended to be geopotential heights and relative vorticity, except in extratropical winter latitudes, when temperature predominated. We believe the choice of temperature for mid-latitude winter equations is related to the greater variation of tropopause height in winter. Climatology is a very important predictor. It accounts for as much as 57% of the variance and was chosen first in three of the six equations. That was expected, considering the strong climatological signal exhibited by total ozone.

The total variance explained ranges from 81.6% for summer northern latitudes to 47.9% for the winter tropics. The variance explained decreases towards the tropics in both summer and winter. This is also consistent with the postulated relationships between synoptic scale ozone variations and meteorological variables. In the tropics, the total ozone variance is smaller to begin with, and also is not as strongly related to upper atmospheric meteorological variables.

Figures 2.1 to 2.6 are predicted-observed scatter diagrams for the dependent sample for the six equations. For ease of depiction, the mean observed values are plotted for 25 Dobson units ranges of forecast values as points at the centres of circles. The area of the circle is proportional to the sample size for each bin. Corresponding standard deviations (SDEV) are plotted at the bottom of each graph, and the total sample size is given in the upper left of each graph, along with the latitude band for which the equation is valid and the root mean square error (RMSE). It can be seen that there is a slight tendency for the extreme values of total ozone, both maxima and minima, to be underpredicted, while values in the middle ranges have been well-fit.

Table 2.1: Predictors chosen by forward stepwise regression.

Predictor	RV	RMSE % DU	Predictor	RV	RMSE % DU
Summer 40-75 degrees north			**Winter 33-75 degrees north**		
CLIMOZ	57.4	27.0	TT400	64.3	32.8
QR150	75.9	20.3	CLIMOZ	74.8	27.5
QR400	77.3	19.7	QR150	77.0	26.4
TT400	80.0	18.5	TT100	77.9	25.8
CORIOLIS	81.6	17.8	CORIOLIS	79.1	25.1
			TT150	79.7	24.8
			TT200	80.8	24.1
			UU150	81.3	23.7
Summer 30-50 degrees north			**Winter 23-43 degrees north**		
GZ250	63.9	19.8	TT100	55.4	23.5
CLIMOZ	68.0	18.1	CLIMOZ	62.0	21.7
QR300	72.5	17.3	CORIOLIS	67.0	20.2
LATDEG	73.4	17.0	GZ100	69.0	19.6
TT100	75.4	16.3	UU100	71.3	18.8
VV150	76.2	16.1	TT250	72.5	18.4
Summer 10-30 degrees north			**Winter 10-23 degrees north**		
CLIMOZ	39.6	12.9	CLIMOZ	33.9	12.0
QR150	49.0	11.9	QR150	40.4	11.4
GZ100	52.0	11.5	TT150	43.7	11.1
UU100	55.5	11.1	GZ100	45.3	10.9
			UU100	47.9	10.6

CLIMOZ	Smoothed climatology	QR	Relative vorticity
TT	Temperature	CORIOLIS	Coriolis parameter
GZ	Geopotential height	LATDEG	Latitude in degrees.
UU and VV	Zonal and meridional wind components		

Pressure levels 100, 150, 200, 250, 300 and 400 are in hPa respectively

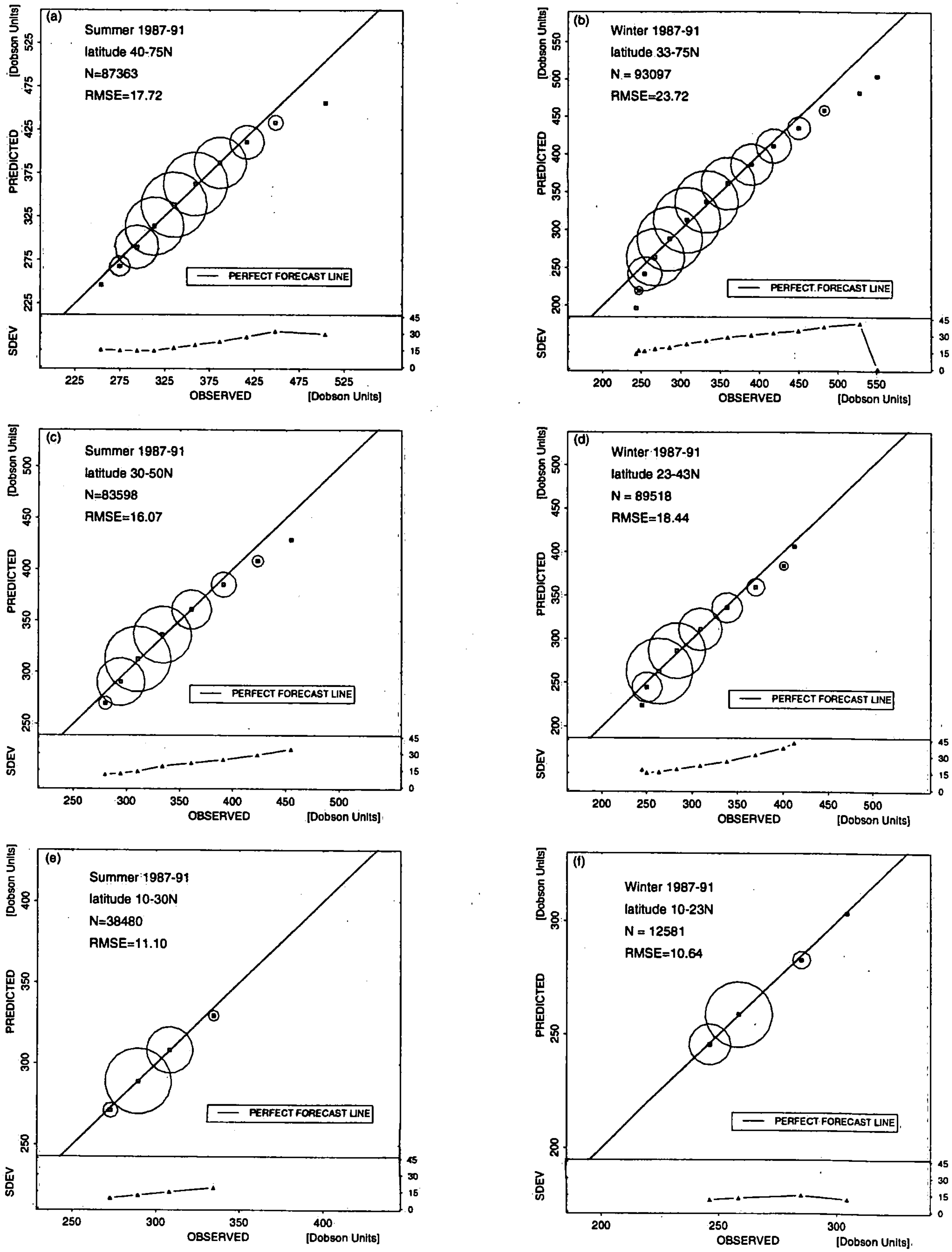

Figure 2.1-2.6: Regression fit. See text for more information.

2.3 Correction procedure

Forecasts from the regression equations are subject to a "correction" procedure, which is based on observations from the Canadian network of 13 Brewer spectrophotometers. The purpose of the correction is to bring current ozone observations into the process, and to correct for the drift of the climatology of ozone. The correction procedure is applied after the statistical forecasts have been made, but before the calculation of the UV index; it is the corrected forecasts that are used in the UV index calculation.

Because of timing considerations, there is a one-day lag in the corrections. That is, yesterday's observations are used to correct forecasts valid today. The correction procedure is also designed to be robust, to use whatever observed data is available. This is due to the fact that the observations from the Brewer network are available only under sunny conditions, thus there will be many missing observations. Furthermore, the observations that are available cover only Canadian areas while the forecast is valid for all of the northern hemisphere. The correction procedure had to be designed to revert smoothly to a valid and reasonable correction away from the data areas. For mid-latitude areas away from Canada, the correction reverts to the average of the corrections at the Canadian stations. For more southern latitudes, the correction reverts linearly to 0, south of 40 degrees N. There are two reasons for this. First, the uncorrected field is probably a better estimate of the ozone in the tropics than the corrected field since the equations for the tropics are different and are designed to explain ozone variations there. Second, the variability of ozone is much higher in mid-latitudes, resulting in higher average corrections, which are unreasonably high for the tropics.

The correction procedure actually consists of an analysis of residuals, where forecast-observed differences are computed at each data point, then a portion of the residual field is added to the forecast. The method is recursive. That is, it is the residual field itself that is updated each day in light of new data. In this way, the system "remembers" previous corrections. Implied in this design is the assumption that the error in the forecast is persistent, for an absence of new data means that the previous day's residual field will be applied again today, unchanged.

The correction procedure also includes a means of computing "surrogate" or "bogus" residuals at stations where there isn't a new observation. The surrogates are weighted averages of yesterday's residual at the site and today's residuals at surrounding points. Yesterday's residual is given a weight equivalent to today's at a point 800km away. The choice of radii of influence for the analysis and the weighting of "old" residuals is supported by temporal correlation studies of ozone, as described below.

Mathematically, the correction procedure works as follows: First, today's residuals are given by equation 2.1:

$$R_n(t_0) = DU(t_0) - OBS(t_0) \qquad (2.1)$$

$(n = 1, \ldots N_0)$

for the N_0 stations where observations are available, where the subscript "0" refers to the current day and the index "n" runs over the station set (currently 13). The surrogate residuals $R_n(t_0)$ are calculated for each of the N_s *stations* where there is no observation as a weighted sum of the residuals at the stations where there is an observation and yesterday's observation at station n,

$$R_n(t_0)=\frac{R_n(t_{-1})*\omega_{MEM}+\sum_{n=1}^{N_0}R_n(t_0)\omega_n}{\omega_{MEM}+\sum_{n=1}^{J}\omega_n}-DCFIELD_n(t_{-1}) \qquad (2.2)$$

$(n = 1,...N_s)$

Since today's residual reflects yesterday's adjustment to the correction field, this must be taken into account when using yesterday's residual, hence the subtraction of *DCFIELD* in equation 2.2. In equation 2.2,

$$\omega_n=\frac{1}{[D_n+XINFL]^{INDW}} \qquad (2.3)$$

$$\omega_{MEM}=\frac{1}{[XMEM+XINFL]^{INDW}} \qquad (2.4)$$

where XINFL and XMEM are the influence radius and "memory" distance respectively. XMEM is currently 800 km, which means that yesterday's observation is considered to be equivalent to today's observation at a distance of 800 km in terms of information content about today's observation at the station. XINFL is used as a sort of minimum influence radius, to help control the occurrence of small scale "bulls eyes" around individual stations. INDW is the exponent of the weighting function. Currently, it is set to 1.0 for linear weighting. Finally, D_n is the distance from the observation sites and the site where a surrogate value is wanted.

Once actual or surrogate residuals are available for all stations, they are analyzed (spread) across the grid by the standard Cressman-type inverse distance-weighted scheme, to produce a new adjustment to the correction field $DCFIELD_{ij}(t_0)$, as:

$$DCFIELD_{ij}(t_0) = \frac{r\sum_{n=1}^{N} R_n \omega_{ij}}{\sum_{n=1}^{N} \omega_{ij}} \qquad (2.5)$$

where the weights ω_{ij} are given by:

$$\omega_{ij} = \frac{1}{[D_{ij} + XINFL]^{INDW}} \qquad (2.6)$$

Again, XINFL is used to control "bulls eyes" around individual stations, and INDW is set to 1.0 for linear distance-weighting. The coefficient "r" is added to control the response in a similar fashion to the response coefficient used in Kalman Filtering. A value of 1.0 means that all of the current discrepancy is added to the correction field, for maximum response to current data. r is currently set to 0.6, a value which gave best accuracy in tests. This value turns out to be close to the serial correlation coefficient for a one-day lag in ozone observations (see section 2.5 below). Use of a value for r of less than 1.0 represents an "undercorrection" - and has the effect of smoothing the response to the current day's data. For points far from Canada (far from all the data points), D_{ij} becomes large and ω_{ij} small and nearly equal over all N stations. Thus $DCFIELD_{ij}(t_0)$ reverts to the average of today's residuals.

One more adjustment to the analysis is needed, because of the variations in residual variance between mid latitudes and the tropics. Since total ozone variations with time are much smaller in the tropics, residuals determined from mid-latitude (Canadian) observations will not be representative of the tropics. In the absence of data in the tropics, we decided to linearly damp the residual field from 39 degrees north to 0 at the equator. This is accomplished by using a weight which varies linearly from 1 at 39 north to 0 at the equator. This means that the forecasts revert to the values given by the equations (uncorrected) in the tropics

The new corrected field becomes,

$$CFIELD_{ij}(t) = CFIELD_{ij}(t_0) + DCFIELD_{ij}(t_0) \qquad (2.7)$$

and the corrected forecast field for the next day is,

$$DU_{ij}(t) = DI_{ij}(t) - CFIELD_{ij}(t) \qquad (2.8)$$

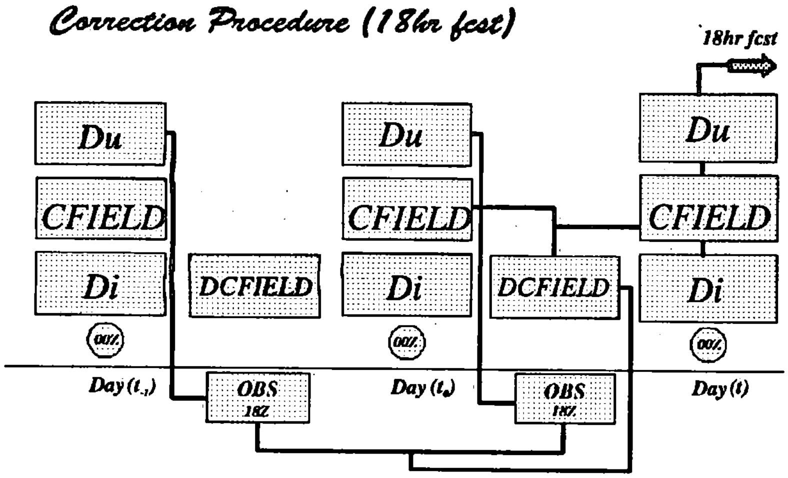

Figure 2.7: Correction procedure for an 18hr fcst.

Figure 2.7 is a schematic of the correction procedure.

2.4 The operational forecast

The previous sections describe the elements of the total ozone forecast procedure. There are six regression equations valid for different latitude bands and for two seasons which are used to generate the initial forecast, and then the forecasts are corrected using the recursive correction procedure. This section describes the way in which the components are put together to generate ozone and UV forecasts.

The new forecast technique has been running at CMC since June 9, 1993. It runs twice a day year round to produce forecasts for the 240 by 60, 1.5 by 1.5 degree hemispheric latitude-longitude grid. Predictor values for the regression equations come from the global spectral model. Each day, the first ozone/UV run is initiated around 04:05 UTC, producing an 18h and a 42h forecast based on the 00:00 UTC model run. Later in the day, the second ozone/UV run is initiated around 19:20 UTC to produce a 30h forecast based on the 12:00 UTC model run. All these forecasts are valid at 18:00 UTC, which is near local solar noon in Canada.

To compute the forecast ozone, first the global model predictors must be interpolated from the model's 360 by 120 global grid to the ozone/UV 240 by 60 grid. The initial forecast for each grid point (DI_{ij}) is computed from the statistical equations, then linearly merged over the latitude boundaries. Furthermore, the forecasts are merged between the two seasons during spring and fall, again linearly. Both blends ensure a soft transition across the latitude and seasonal boundaries of the equations. The temporal merging is from September 1 to October 11 and between March 27 and May 4. The current date is transformed to the Julian day (t_{JD}) and the following formula accomplishes the merge:

$$DI(t_{JD}) = \omega_{temp}(t_{JD}) SUMMER_{REG} + (1 - \omega_{temp}(t_{JD}) WINTER_{REG}) \qquad (2.9)$$

Table 2.2 summarizes the way in which the regressions are used.

Table 2.2: Regression used over different latitude belts.

REGRESSION	LATITUDE	ω_{apd}	REGRESSION	LATITUDE	ω_{apd}
Summer 40-75 degree N	53.0N to 89.0N	1	**Winter 33-75 degrees N**	45.5N to 89.0N	1
Summer 40-75 degree N + Summer 30-50 degrees N	41.0N to 51.5N	1 → 0 0 → 1	Winter 33-75 degrees N + Winter 23-43 degrees N	33.5N to 44.0N	1 → 0 0 → 1
Summer 30-50 degree N	36.5N to 39.5N	1	**Winter 23-43 degrees N**	29.0N to 32.0	1
Summer 30-50 degrees N + Summer 10-30 degrees N	24.5N to 35.0N	1 → 0 0 → 1	Winter 23-43 degrees N + Winter 10-23 degrees N	17.0N to 27.5N	1 → 0 0 → 1
Summer 10-30 degrees N	0.5N to 23.0N	1	**Winter 10-23 degrees N**	0.5N to 15.5N	1

The steps of the operational forecast procedure are as follows (see figure 2.7 for a pictorial representation of the forecast procedure):

For the 18 hour forecast for tomorrow (t_{+1}):

1. Compile today's final ozone forecast field ($DU_{18}(t_0)$) and today's observations ($OBS_{18}(t_0)$). Today's final forecast is generated from today's 00:00 UTC model run and is valid today at 18:00 UTC.
2. For computation of surrogate residuals, compile yesterday's observations ($OBS_{18}(t_{-1})$) and yesterday's final forecast field ($DU_{18}(t_{-1})$), as generated from yesterday's 00:00 UTC run and valid yesterday at 18:00 UTC.
3. Compute today's residuals and surrogate residuals from 1 and 2 and today's delta correction field ($DCFIELD_{18}(t_0)$).
4. Run the equations on tomorrow's 00:00 UTC model data (the run actually happens about 04:05 UTC) to obtain tomorrow's initial forecast ($DI_{18}(t_{+1})$).
5. Update the correction field by adding today's delta correction field, to give tomorrow's correction field ($CFIELD_{18}(t_{+1})$).
6. Compute tomorrow's 18 h forecast by adding the updated correction field to the initial forecast.

For the 42 h forecast (t_{+2}):

1. Compile today's final ozone forecast field ($DU_{42}(t_0)$) and today's observations ($OBS_{18}(t_0)$). Today's final forecast is generated from yesterday's 00:00 UTC model run and is valid today at 18:00 UTC.
2. For computation of surrogate residuals, compile yesterday's observations ($OBS(t_{-1})$) and yesterday's final forecast field ($DU_{42}(t_{-1})$), as generated from the day before yesterday's 00:00 UTC run and valid yesterday

at 18:00 UTC.
3. Compute today's residuals and surrogate residuals from 1 and 2 and today's delta correction field ($DCFIELD_{42}(t_0)$).
4. Run the equations on tomorrow's 00:00 UTC model data (the run actually happens about 04:05 UTC) to obtain the day after tomorrow's initial forecast ($DI_{42}(t_{+2})$).
5. Update the correction field by adding today's delta correction field, to give tomorrow's correction field ($CFIELD_{42}(t_{+2})$).
6. Compute the day after tomorrow's 42 h forecast by adding the updated correction field to the initial forecast.

For the 30 h forecast (t_{+1}):

1. Compile today's final ozone forecast field ($DU_{30}(t_0)$) and today's observations ($OBS_{18}(t_0)$). Today's final forecast is generated from yesterday's 12:00 UTC model run and is valid today at 18:00 UTC. The run is started later in the day to try to catch today's observations.
2. For computation of surrogate residuals, compile yesterday's observations ($OBS_{18}(t_{-1})$) and yesterday's final forecast field ($DU_{30}(t_{-1})$), as generated from the day before yesterday's 12:00 UTC run and valid yesterday at 18:00 UTC.
3. Compute today's residuals and surrogate residuals from 1 and 2 and today's delta correction field ($DCFIELD_{30}(t_0)$).
4. Run the equations on today's 12:00 UTC model data (the run actually happens about 19:20 UTC) to obtain tomorrow's initial forecast ($DI_{18}(t_{+1})$).
5. Update the correction field by adding today's delta correction field, to give tomorrow's correction field ($CFIELD_{30}(t_{+1})$).
6. Compute tomorrow's 30 h forecast by adding the updated correction field to the initial forecast.

After the final forecasts are made, Kerr's UV flux equation (equation 1.1), is applied, using the local solar noon zenith angle (a function of latitude only) and the forecast ozone values to compute the UV index. Figures 2.8 to 2.11 show an example of the initial forecast, (*DI*), the corrected forecast (*DU*), the correction field (*CFIELD*) and the corresponding UV index, for June 1, 1993. In addition to the maps of the UV index under clear sky conditions, point UV forecasts (under clear skies) are also obtained for Canadian cities, and are included in CMC's FXCN20's bulletins. These bulletins consist of a categorical UV forecast related to the times of day when the UV index will be above 4.0, according to the diurnal variation of zenith angle. Also, there is a FPCN48 bulletin (49 in french), as shown in table 2.3 as an example. This bulletin includes the weather forecast (from the regions), and a categorical UV forecast related to the sky condition and the times of day. When rain (or snow) is forecast, an estimated reduced value (0.4) of the index is inserted in place of the clear sky noon value. Under heavy clouds, a reduced value of 0.7 is used, otherwise there is no reduced value under other sky conditions.

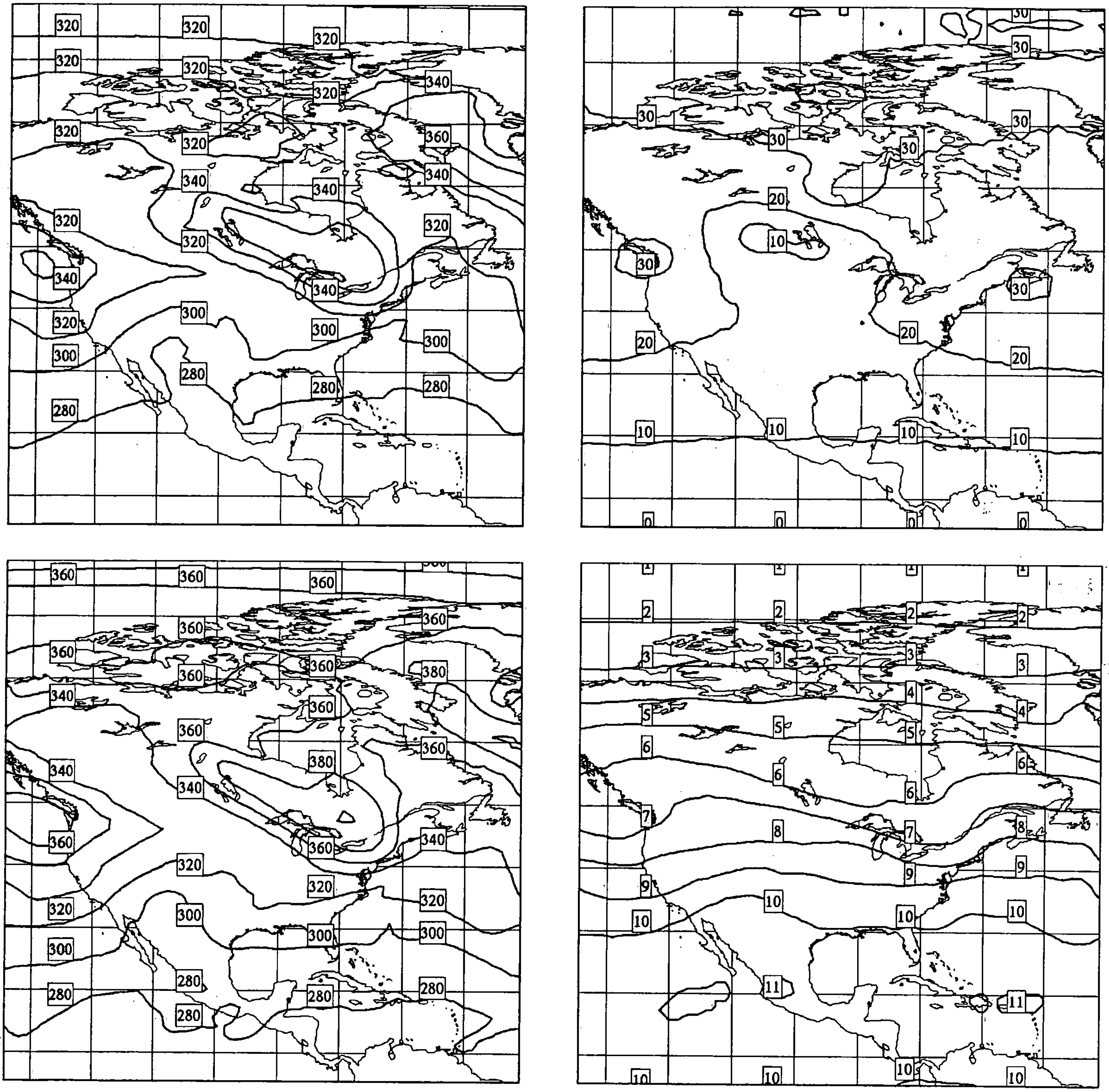

Figure 2.8 to 2.11: 1 June 1993, 18hr fcst. Respectively ozone initial (*DI*), correction (*DFIELD*) and ozone final (*DU*) in DU. Finally the UV index.

Table 2.3: The FPCN48 issued at CMC.

FPCN48 CWAO 090745
ENVIRONMENT CANADA FORECAST ULTRAVIOLET (UV) INDICES FOR SELECTED CANADIAN CITIES FOR FRIDAY JULY 09 1993. THE UV INDEX BULLETIN IS ISSUED TWICE DAILY EVERY 12 HOURS.

THE FORECAST UV INDEX GENERALLY INDICATES THE UV INTENSITY IN FULL SUNLIGHT AT MIDDAY. ULTRAVIOLET INTENSITIES ARE LOWER UNDER THICK CLOUD COVER AND/OR PRECIPITATION.

VARIABLE CLOUD DAYS ALLOW FULL ULTRAVIOLET EXPOSURE DURING THE SUNNY PERIODS.

LOCATION	WEATHER	FCST UV INDEX	CATEGORY	TIMES UV ABOVE 4.0
IQALUIT	CLOUDY	4.7	MODERATE	11 TO 2
RESOLUTE	CLOUDY PERIODS	3.0	LOW	NIL
INUVIK	SUNNY	4.2	MODERATE	2 TO 4
RANKIN INLET	MAINLY CLOUDY	4.8	MODERATE	11 TO 3
YELLOWKNIFE	MAINLY SUNNY	5.0	MODERATE	12 TO 4
WHITEHORSE	PARTLY CLOUDY	5.4	MODERATE	12 TO 4
VANCOUVER	SUNNY	6.8	MODERATE	10 TO 4
VICTORIA	SUNNY	6.9	MODERATE	10 TO 4
KAMLOOPS	SHOWERS	*5*	MODRT DUE CLD/PRECIP	11 TO 3
NANAIMO	SUNNY	6.8	MODERATE	10 TO 4
PORT HARDY	MAINLY CLOUDY	6.5	MODERATE	11 TO 4
SANDSPIT	MAINLY SUNNY	6.0	MODERATE	11 TO 4
PRINCE RUPERT	MAINLY SUNNY	6.0	MODERATE	11 TO 4
KELOWNA	SHOWERS	*5*	MODRT DUE CLD/PRECIP	11 TO 3
PRINCE GEORGE	CLOUDY	6.0	MODERATE	11 TO 4
CRANBROOK	SHOWERS	*5*	MODRT DUE CLD/PRECIP	11 TO 3
CASTLEGAR	SHOWERS	*5*	MODRT DUE CLD/PRECIP	11 TO 3
EDMONTON	CLOUDY	6.6	MODERATE	11 TO 4
CALGARY	CLOUDY	6.9	MODERATE	11 TO 5
LETHBRIDGE	MAINLY CLOUDY	7.0	HIGH	11 TO 5
GRANDE PRAIRIE	CLOUDY	6.5	MODERATE	11 TO 5
SASKATOON	FEW SHOWERS	6.4	MODERATE	10 TO 4
REGINA	FEW SHOWERS	7.0	HIGH	10 TO 4
YORKTON	FEW SHOWERS	6.8	MODERATE	10 TO 4
THOMPSON	MAINLY CLOUDY	6.0	MODERATE	11 TO 4
WINNIPEG	PARTLY CLOUDY	6.8	MODERATE	10 TO 4
THUNDER BAY	VARIABLE CLOUD	7.2	HIGH	11 TO 5
SUDBURY	FEW SHOWERS	8.4	HIGH	10 TO 5
WINDSOR	HAZY	9.2	EXTREME	10 TO 5
TORONTO	FEW SHOWERS	8.9	HIGH	10 TO 5
BARRIE	ISOLATED SHOWERS	8.8	HIGH	10 TO 5
LONDON	FEW SHOWERS	9.0	EXTREME	10 TO 5
OTTAWA	OCCASIONAL RAIN	*6*	MODRT DUE CLD/PRECIP	10 TO 4
MONTREAL	OCCASIONAL RAIN	*6*	MODRT DUE CLD/PRECIP	10 TO 4
SHERBROOKE	VARIABLE CLOUD	8.5	HIGH	9 TO 4
QUEBEC	VARIABLE CLOUD	8.3	HIGH	9 TO 4
STE-ADELE	OCCASIONAL RAIN	*6*	MODRT DUE CLD/PRECIP	10 TO 4
FREDERICTON	VARIABLE CLOUD	8.1	HIGH	10 TO 5
SAINT JOHN NB	VARIABLE CLOUD	8.2	HIGH	10 TO 5
HALIFAX	VARIABLE CLOUD	8.3	HIGH	10 TO 5
CHARLOTTETOWN	VARIABLE CLOUD	7.9	HIGH	10 TO 5
ST JOHNS NFLD	OCCASIONAL RAIN	*5*	MODRT DUE CLD/PRECIP	11 TO 3
GOOSE BAY	CLOUDY PERIODS	6.4	MODERATE	10 TO 4

* ESTIMATE OF UV UNDER CLOUD AND/OR PRECIPITATION *

ALL TIMES MENTIONED IN THIS BULLETIN ARE IN LOCAL TIME.

SUN TIP:
IT S NOT COOL TO BURN, APPLY A BROAD SPECTRUM SUNSCREEN WITH A SUN PROTECTION FACTOR OF AT LEAST 15.

UV CATEGORIES	UV INDEX RANGE	AVERAGE TIME TO BURN
EXTREME	9.0 OR HIGHER	LESS THAN 15 MINUTES
HIGH	7.0 TO 8.9	AROUND 20 MINUTES
MODERATE	4.0 TO 6.9	AROUND 30 MINUTES
LOW	LESS THAN 4.0	ONE HOUR OR MORE

NOTE: AVERAGE TIME TO BURN ONLY ADDRESSES UV EFFECTS ON THE SKIN. UV ALSO AFFECTS THE EYES.

THIS BULLETIN WILL NOT BE AMENDED. CONTACT YOUR LOCAL ENVIRONMENT CANADA WEATHER OFFICE TO OBTAIN THE MOST UP-TO-DATE WEATHER AND UV INDEX INFORMATION

2.5 Serial correlation study

To support the choice of parameters in the correction procedure, we carried out a residuals lag correlation study on the 1993 observation data. Such a correlation study gives an idea of the relative information content in today's residual to predict tomorrow's residual. The greater the correlation for a one-day lag, the greater the dependence of tomorrow's error on today's error. The form of the linear correlation coefficient for a lag of d days in variable X is,

$$\rho = \frac{cov(X,X_{-d})}{S_X S_{X_{-d}}} \tag{2.10}$$

where cov is the covariance and S represents the standard deviation. As applied to the residuals, the lag autocorrelation for d days is given by,

$$r_d = \frac{\sum_{j=1}^{J}\sum_{n=1}^{N}(R_{jn}-\bar{R})(R_{jn_{-d}}-\bar{R}_{-d})}{JN\sqrt{\frac{\sum_{j=1}^{J}\sum_{n=1}^{N}(R_{jn}-\bar{R})^2}{JN}}\sqrt{\frac{\sum_{j=1}^{J}\sum_{n=1}^{N}(R_{jn_{-d}}-\bar{R}_{-d})^2}{JN}}} \tag{2.11}$$

for J stations and N consecutive days. The overbar denotes a mean over the entire sample. As d increases, one would expect the correlation to decrease. The slower the decrease, the longer the "memory" of a given residual. Figure 2.12 shows the autocorrelation coefficients as a function of lag in days for each station separately and for all stations. The figure indicates that average 1 day lag correlation is 0.72 and two day lag correlation is 0.64. The system presently feeds back 60% of the residual for all forecasts. The lag correlation study suggests this value could be increased slightly for the 18h and 30h (one day) forecasts, but is reasonable for the 42h (two day) forecasts. Finally, it should be noted that the correlation estimate is based on a relatively small sample consisting of cases where consecutive 1 day or 2 day observations were available. Correlations might also vary regionally, but the small sample collected so far cannot support regional stratification. Correlations might also be lower in winter because of the greater variance in wintertime ozone and because of greater RMSE of the forecast system.

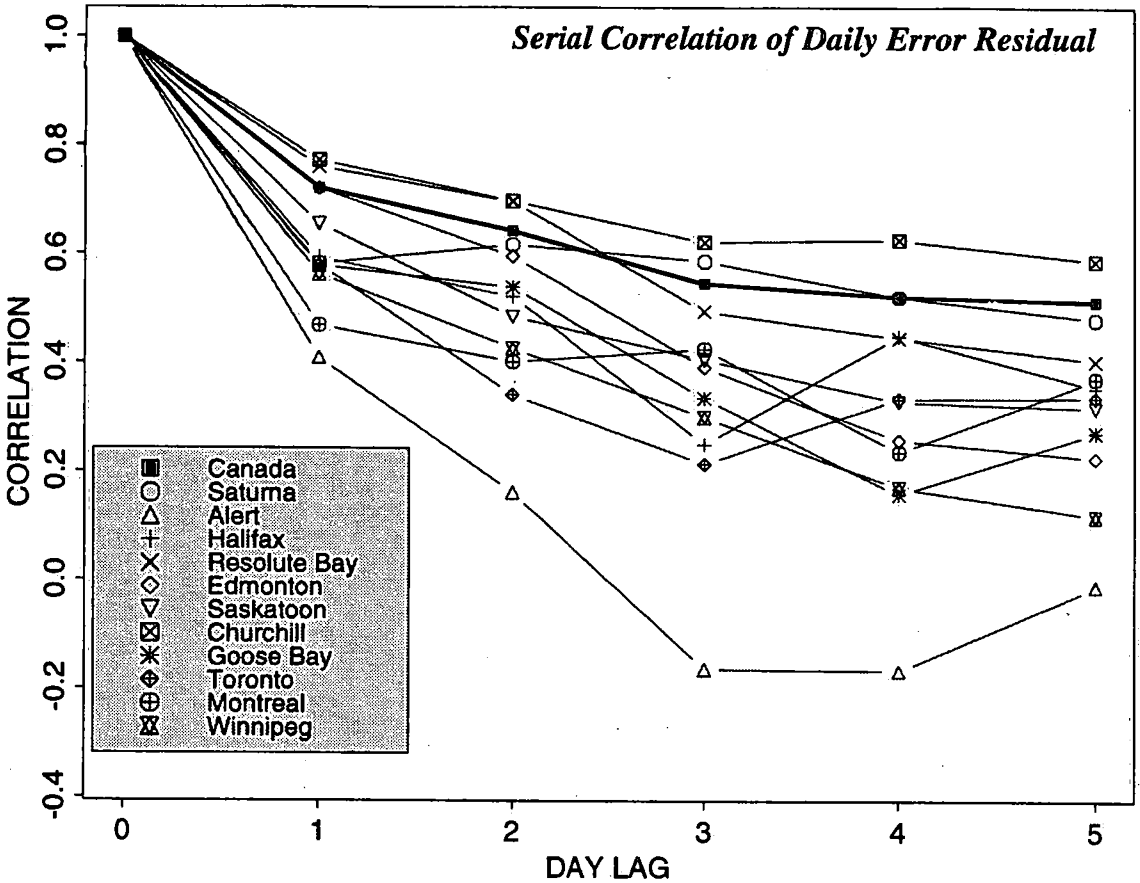

Figure 2.12: Serial correlation for 11 brewer locations, based on all available data for summer 1992 and summer 1993.

▸ Chapter Three ◂
EVALUATION OF THE OZONE AND UV INDEX FORECASTS

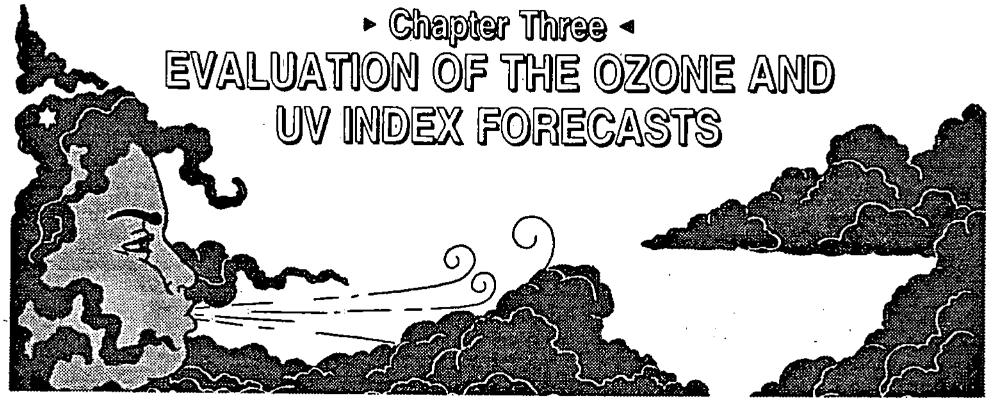

3.1 Comparison between the previous and the new statistical technique

The technique described in this report contains several improvements over the first ozone forecast technique that was applied operationally in 1992. The main improvements are:

1. The 1993 technique uses a quantitative multiple linear regression formulation between many atmospheric variables and total ozone, based on 5 years of data. The 1992 technique was designed using visual comparisons of 500 mb fields and ozone charts on a few days in April, along with an annual average ozone profile for Edmonton, expressed as a function of potential temperature.

2. The 1993 technique uses observations for all of the valid area of the forecasts, the northern hemisphere. The 1992 technique uses only a selection of data from the Canadian Brewer sites.

3. The 1993 correction procedure is more sophisticated, being recursive and based on a larger observation set.

4. Daily climatological ozone data has been included in the 1993 technique as a basis. Other than the single average Edmonton sounding, no climatological data has been used in the 1992 technique.

Details of the 1992 technique are contained in Wilson et. al., 1992.

With all these improvements, we expected the 1993 technique to perform better than the 1992 technique. To quantify this, we carried out an independent test of the 1993 technique on the 1992 summer and compared the results with those obtained from the operational technique from 1992. The data period is June 2 to August 31, 1992, for which there are a total of 342 Brewer observations available from 10 sites. The 18h forecasts were compared on this dataset. Results of the comparison are summarized in the bargraph (figure 3.1). The most striking improvement shown by figure 3.1 is the dramatic change in the bias of the initial forecasts. Without the quantitative statistical analysis, it proved difficult to obtain a representative

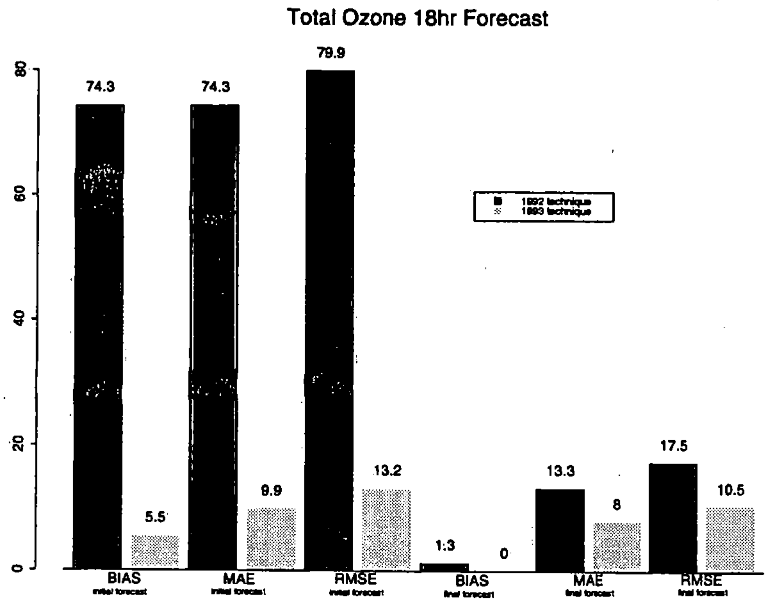

Figure 3.1: Test results comparing the previous technique (1992) and the new technique (1993). Test was done from June 2 to August 31, 1992.

relationship between ozone and meteorological variables in 1992, and the forecasts were biased by 74 DU. The 1993 procedure run on 1992 data produced a bias of 5.5 DU, which can be attributed to depletion of total ozone between the development dataset (centered on 1989) and 1992. Both the MAE and the RMSE have been correspondingly reduced in the initial forecasts.

Both the 1992 and 1993 correction procedures do a good job of removing the bias; final forecasts from both techniques are essentially unbiased. However, the final forecasts from the 1993 procedure are associated with lower MAE and RMSE than the 1992 final forecasts. Since the bias has been removed in both, this improvement can be attributed both to the lower RMSE and MAE in the initial forecasts and to the improved effect of the correction procedure. In fact, RMSE of the initial forecast using the 1993 technique is smaller than the RMSE of the final forecast using the 1992 technique.

3.2 Evaluation of the technique for the summer of 1993

In this section, we present a summary evaluation of the performance of the 1993 technique during the summer of 1993. This represents an evaluation of the operational forecasts for 1993. The verification dataset comes entirely from the Canadian network of Brewer spectrophotometers, which was expanded to 13 sites in 1993. Sufficient data for verification purposes was available from 11 of these stations. The data period is May 4 to September 1, and a total of 965 daily observations were available for the verification. The results are presented first for each station and then are summarized over all stations. Verification statistics are the bias (mean error), mean absolute error (MAE), the root mean square error (RMSE) and the RMSE with the sample bias removed (RMSEcmc). It also includes the climatology and the persistance if they where used as a forecast. The verification was carried out for the initial and final forecasts, and for the 18h and 42h

Table 3.1: Evaluation of the of the 1993 ozone forecast technique.

	Initial forecast				Corrected forecast				CLIM	PER
	Bias	MAE	RMSE $RMSE_{CMC}$	PC (N)	Bias	MAE	RMSE $RMSE_{CMC}$	PC (N)	RMSE $RMSE_{CMC}$	RMSE
	DU	DU	DU	%	DU	DU	DU	%	DU	DU
18hr projection forecast										
Saturna: Sample size= 107	21.2	29.1	32.0	60.0	0.1	8.0	10.7	55.8	36.6	15.5
Mean=313.9 DU, SDEV= 21.2 DU			13.3	(95)			10.7	(95)	22.9	
Edmonton: Sample size= 94	20.6	20.7	23.9	54.4	0.3	8.5	10.5	49.4	36.6	12.5
Mean= 305.8 DU, SDEV= 17.6 DU			12.0	(79)			10.5	(79)	20.9	
Saskatoon: Sample size= 99	11.4	12.2	15.9	55.2	-0.1	7.5	9.7	55.2	27.6	15.3
Mean= 316.7 DU, SDEV= 21.4 DU			11.0	(87)			9.7	(87)	19.7	
Churchill: Sample size= 89	28.5	28.5	31.3	55.1	0.5	8.1	11.2	59.4	43.3	15.2
Mean= 3213.5 DU, SDEV= 26.6 DU			12.9	(69)			11.1	(69)	20.7	
Winnipeg: Sample size= 98	4.8	10.6	14.0	61.8	0.2	8.7	11.5	57.3	21.5	15.7
Mean= 327.3 DU, SDEV= 22.1 DU			13.2	(89)			11.5	(89)	19.5	
Toronto: Sample size= 110	12.4	13.9	17.1	61.4	-0.4	7.9	10.2	53.5	29.5	13.1
Mean= 313.3 DU, SDEV= 23.9 DU			11.8	(101)			10.2	(101)	19.6	
Montreal: Sample size= 87	14.0	15.2	18.0	62.0	-0.9	7.4	9.4	57.8	29.7	17.0
Mean= 320.8 DU, SDEV= 26.5 DU			11.3	(71)			9.4	(71)	22.7	
Goose Bay: Sample size= 76	11.2	15.1	19.0	68.5	0.5	10.4	14.3	59.3	30.9	14.5
Mean = 337.7 DU, SDEV= 25.7 DU			15.3	(54)			14.2	(54)	20.9	
Halifax: Sample size= 80	10.4	14.4	18.0	60.7	-1.7	8.8	11.4	57.1	26.1	15.1
Mean= 325.2 DU, SDEV= 18.9 DU			14.7	(56)			11.3	(56)	19.4	
Alert: Sample size= 33	23.6	23.6	27.7	48.3	1.3	13.2	15.8	41.4	39.0	17.6
Mean= 336.1 DU, SDEV= 41.4 DU			14.5	(29)			15.8	(29)	16.6	
Resolute Bay: Sample size= 92	27.3	27.3	29.3	57.3	-0.1	7.3	9.1	56.1	46.5	12.0
Mean= 316.3 DU, SDEV= 29.5 DU			10.7	(82)			9.1	(82)	22.6	
Canada: Sample size= 965	17.4	19.0	23.0	59.0	-0.1	8.4	11.0	55.3	33.9	14.7
Mean= 319.1 DU, SDEV= 25.9DU			15.2	(812)			11.0	(812)	22.4	
42hr projection forecast										
Saturna	26.9	27.4	31.2	64.2	0.3	9.1	13.0	59.0	36.6	21.6
			15.8	(95)			13.0	(95)	22.9	
Edmonton	20.2	20.5	24.6	48.1	0.4	10.5	13.5	49.4	36.6	18.1
			14.0	(79)			13.5	(79)	20.9	
Saskatoon	11.5	12.8	16.4	58.6	-0.1	8.9	11.7	55.2	27.6	21.4
			11.7	(87)			11.7	(87)	19.7	
Churchill	28.1	28.2	31.2	60.9	-0.1	9.9	12.4	56.5	43.3	18.8
			13.6	(69)				(69)	20.7	
Winnipeg	4.4	9.7	13.4	58.4	-0.4	9.7	12.7	58.4	21.5	20.8
			12.6	(89)			12.7	(89)	19.5	
Toronto	12.5	14.2	17.9	56.4	-0.7	8.8	11.8	52.5	29.5	18.3
			12.9	(101			1189	(101)	19.6	
Montreal	15.5	16.7	19.8	49.3	-1.7	8.1	11.1	57.8	29.7	19.7
			12.3	(71)			11.0	(71)	22.7	
Goose Bay	10.4	15.7	20.3	72.2	-1.0	13.7	18.5	64.8	30.9	24.1
			17.4	(54)			18.5	(54)	20.9	
Halifax	11.6	15.6	19.1	60.7	-1.3	10.1	13.0	60.7	26.1	20.0
			15.2	(56)			13.0	(56)	19.4	
Alert	22.0	22.1	26.7	41.4	3.2	13.1	17.1	48.3	39.0	21.2
			15.2	(29)			16.8	(29)	16.6	
Resolute Bay	26.6	26.6	29.3	48.8	0.4	10.2	12.4	48.8	46.5	15.6
			12.4	(82)			12.4	(82)	22.6	
Canada	17.1	18.9	23.3	56.8	-0.3	9.9	13.2	55.5	33.9	19.9
			15.9	(812)			13.2	(812)	22.4	

projections based on 00:00 UTC model data.

Table 3.1 shows the summary verification statistics for each station and for the 18 and 42h forecast. projections based on 00:00 UTC model data. Biases in 1993 were below 15 DU at 6 of the 11 stations, and above 20 DU at the other 5. Higher biases for the northern stations Resolute and Alert may be caused by unrepresentativeness in the development sample, and perhaps to inaccuracies of the TOMS data at low sun angles. We are not sure why the bias would be relatively high at the three stations Saturna, Edmonton and Churchill. Bias levels at all stations are higher in 1993 than in 1992 (see section 3.1) because of the anomalously low levels of ozone observed in the spring and early summer at all stations. This anomaly is believed to be caused by non-meteorological processes, and therefore would not be caught by the meteorological predictors. Averaged over all stations, the bias is 17.4 DU in 1993, compared to 5.5 DU in 1992.

The correction procedure does a very good job of removing the bias in the forecasts, for 1993 and 1992 data. After correction, the highest bias at any station is 1.7 DU. It should be noted in this context that the correction procedure would be expected to correct whatever bias is measured in the verification because the same dataset was used for verification as was used in the correction procedure, albeit offset by one day. The remaining bias in the corrected forecasts can be attributed to the effects of the one-day offset in the application of the correction, and to the fact that only part of the correction is applied each day.

The RMSEcmc statistics of table 3.1 give an indication of the random (unexplained) component of the variation in the observed ozone. Values are consistent over all stations, ranging from 11 to 15 DU for the uncorrected 18h forecasts and 9 to 14 DU for the corrected 18h forecasts, and slightly higher for the 42h forecasts. With the exception of Alert, the RMSEcmc was lowered at all stations by the correction procedure. This means that the correction procedure was able to remove some of the variable component of the error as well as correcting the bias.

The percentage correct (PC) values given in Table 3.1 give an indication of the ability of the technique to correctly forecast changes in total ozone form one day to the next. The PC values are for a three-category contingency table, where the three categories are, 1. decrease in total ozone greater than 2 DU, 2. a change less than or equal to 2 DU, and 3. increase of greater than 2 DU. With these rather stringent limits, the uncorrected forecasts averaged 59% correct at 18h and 57% correct at 42h. The correction procedure slightly degraded the technique's ability to correctly forecast the changes, down to 55% and 55% respectively. We attribute this effect to the one-day offset in the use of observations to correct the forecasts.

A comparison with climatology and persistance (table 3.1) gives an indication whether there is skill in the forecast. It can be seen that the 1993 initial forecasts improve considerably over climatology according to all measures. For example, the uncorrected forecast RMSE level is only about 2/3 the climatological level and the final forecast RMSE is only about 1/3 that of the climatological forecast. One day persistance forecast is slightly better than the initial 18hr forecast when the bias has been removed. Otherwise, the initial 42hr and, the final 18hr and 42hr forecasts are noticeably more skillful than climatology and persistance.

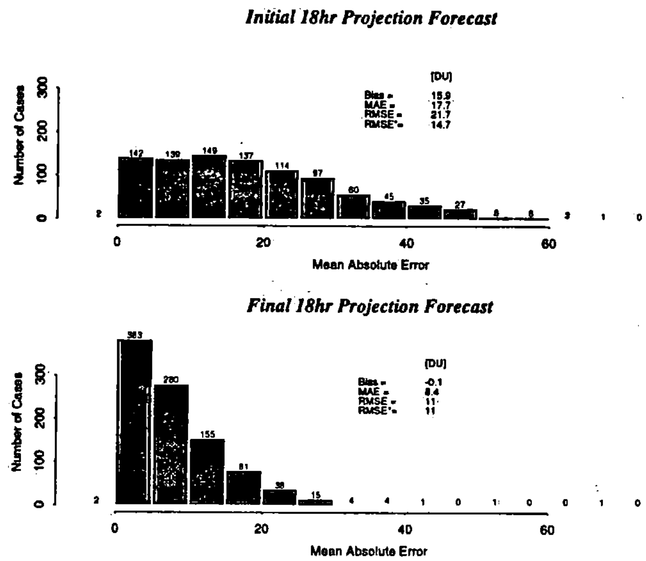

Figure 3.2: Mean absolute distribution error of the 18hr forecast.

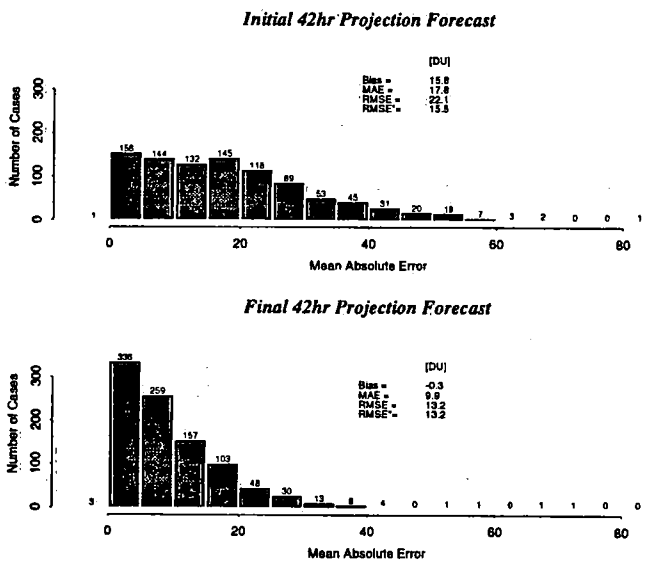

Figure 3.3: Mean absolute distribution error of the 42hr forecast.

Figures 3.2 (for the 18h forecasts) and 3.3 (for the 42h forecasts) present the summary performance results in a slightly different way. Histograms for the initial and final forecasts show the distribution of errors over all Canadian stations, separated into 5 DU bins. The histograms show that about 60% of the initial forecasts were correct to within 20 DU, for both the 18h and 42h projections.

Figures 3.4 to 3.25 consist of timeseries of the ozone forecasts and observations (even numbered figures) and the UV index forecasts and observations (odd-numbered figures), for each station. The ozone observations are the same ones used in the summary verification, that is, the total ozone reported by the Brewer instrument each day. The timeseries plots show clearly the tendency towards overforecasting the ozone in the initial forecasts, and they also show the tendency toward abnormally low ozone values during the first half of the summer, especially at Edmonton, Saturna and Toronto. For comparison purposes a table of summary statistics is once again included for the initial and final forecasts.

The UV index "measurements" are computed from Brewer measurements of UV by applying the index formula to the UV measurements. The measurements are the highest reported UV value for the day from each site. Of course when cloudy conditions occur near solar noon, the maximum value will be reduced, and such "cloudy day" measurements show up as low-valued "spikes" on the graphs. The forecast values are the clear sky, solar noon values produced by the technique; there is no attempt to correct for cloudy conditions. The graphs must therefore be interpreted carefully. At least it is possible to identify the cases of most concern - those days when the forecast UV is lower than the observed value. These are reported

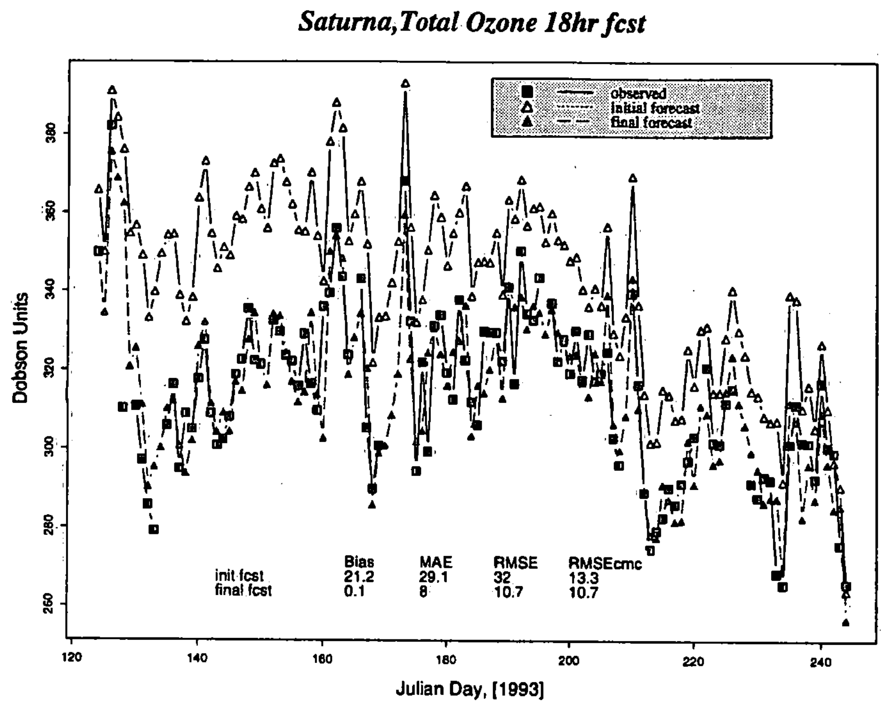

Figure 3.4: Timeseries of total ozone.

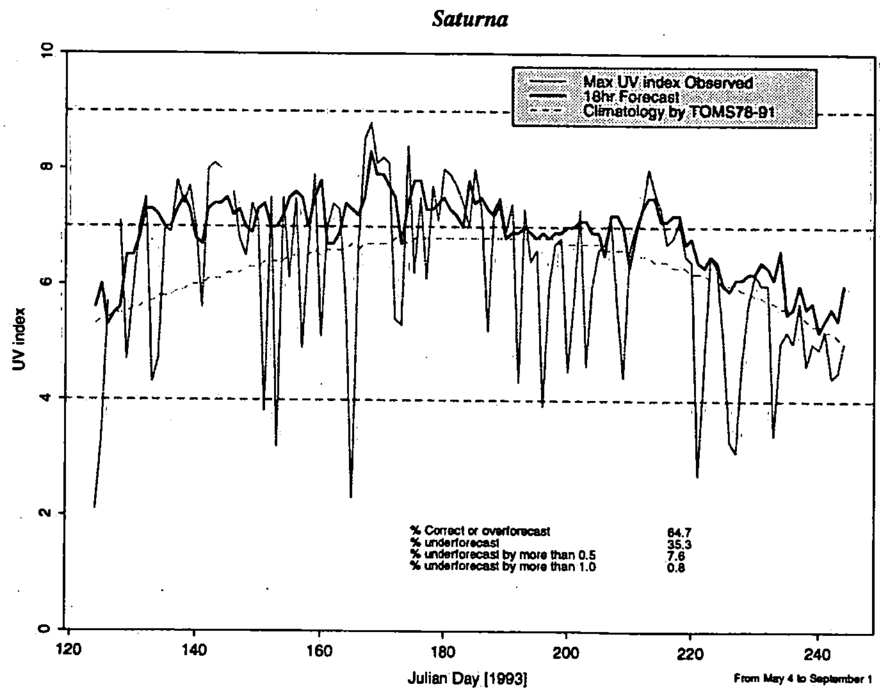

Figure 3.5: Timeseries of UV index.

Edmonton, Total Ozone 18hr fcst

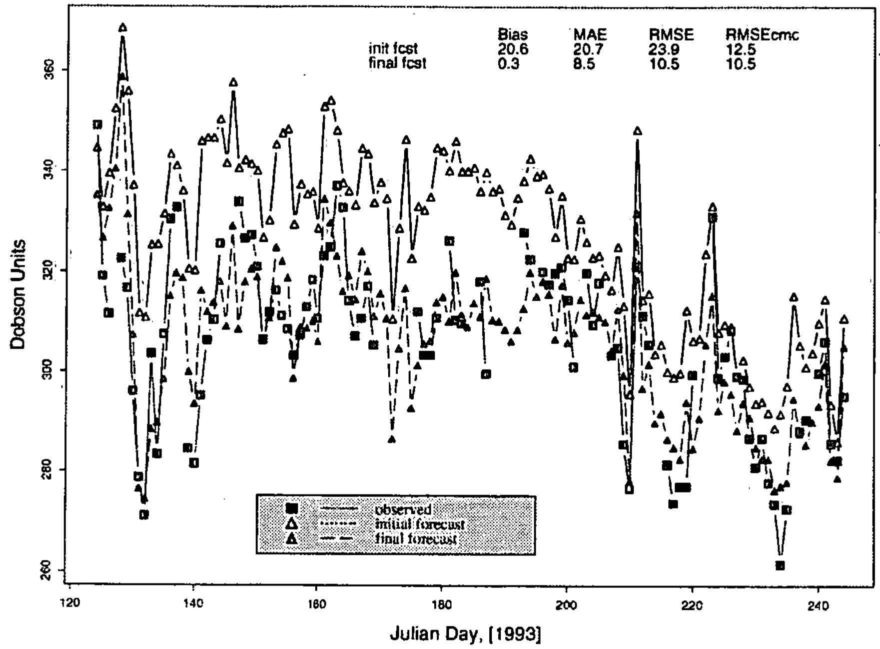

Figure 3.6: Timeseries of total ozone.

Edmonton

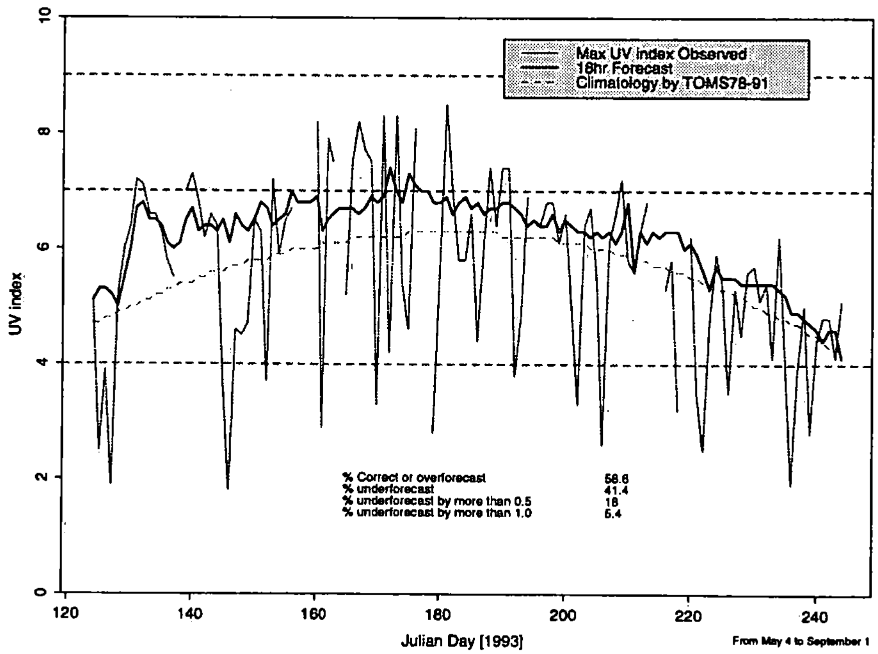

Figure 3.7: Timeseries of UV index.

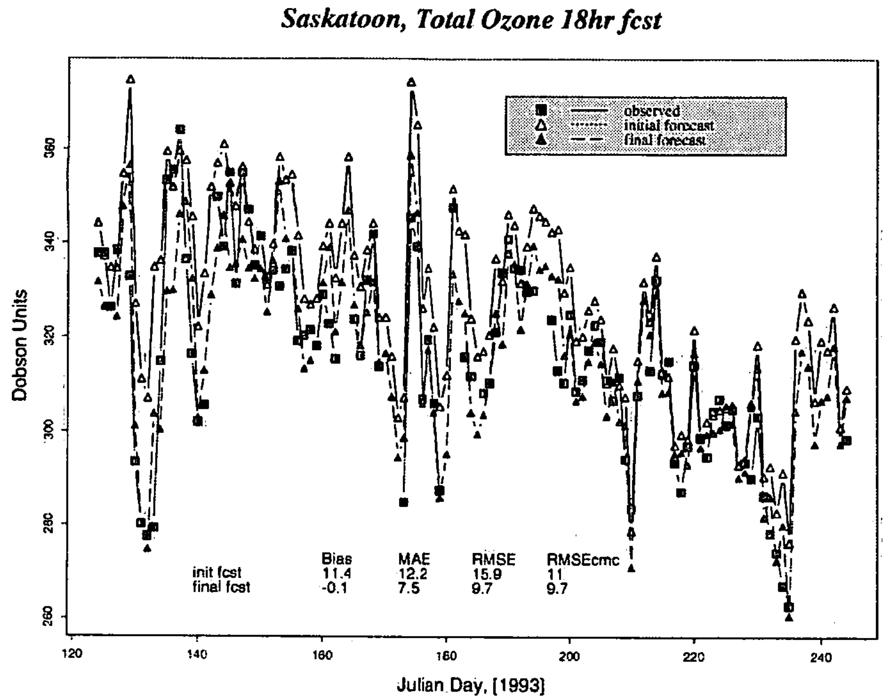

Figure 3.8: Timeseries of total ozone.

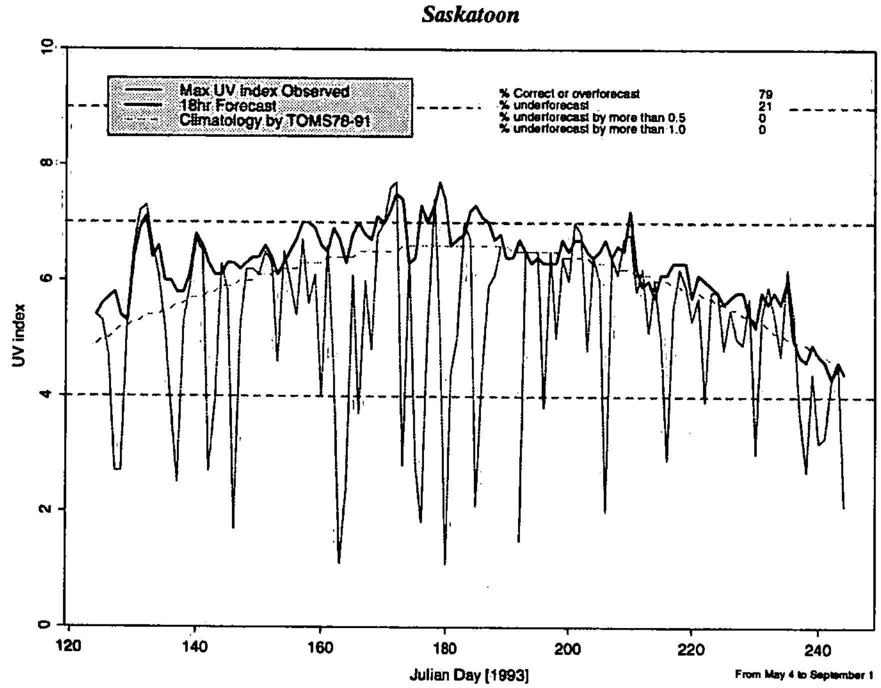

Figure 3.9: Timeseries of UV index.

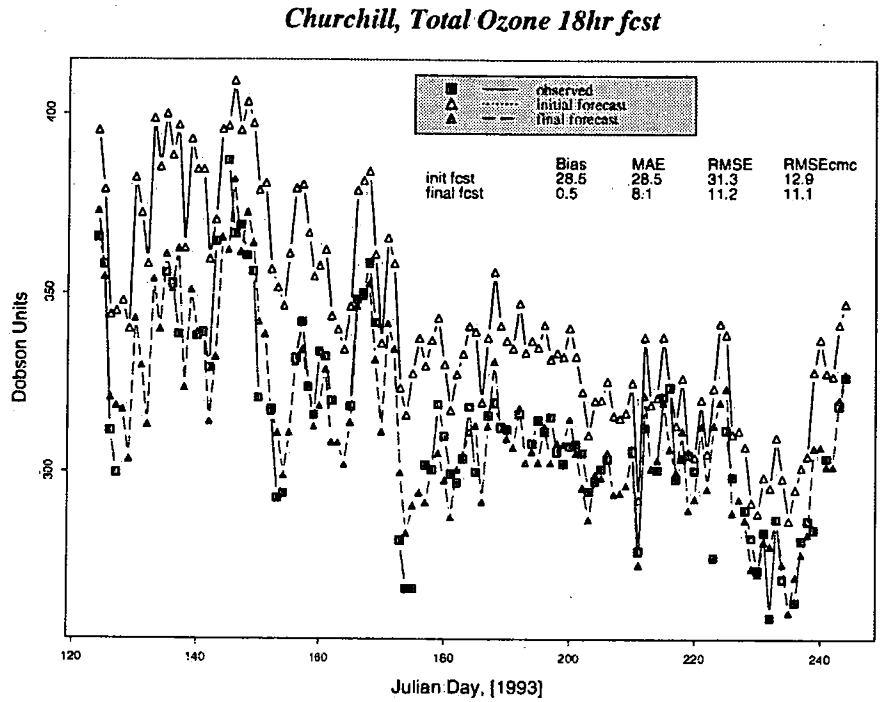

Figure 3.10: Timeseries of total ozone.

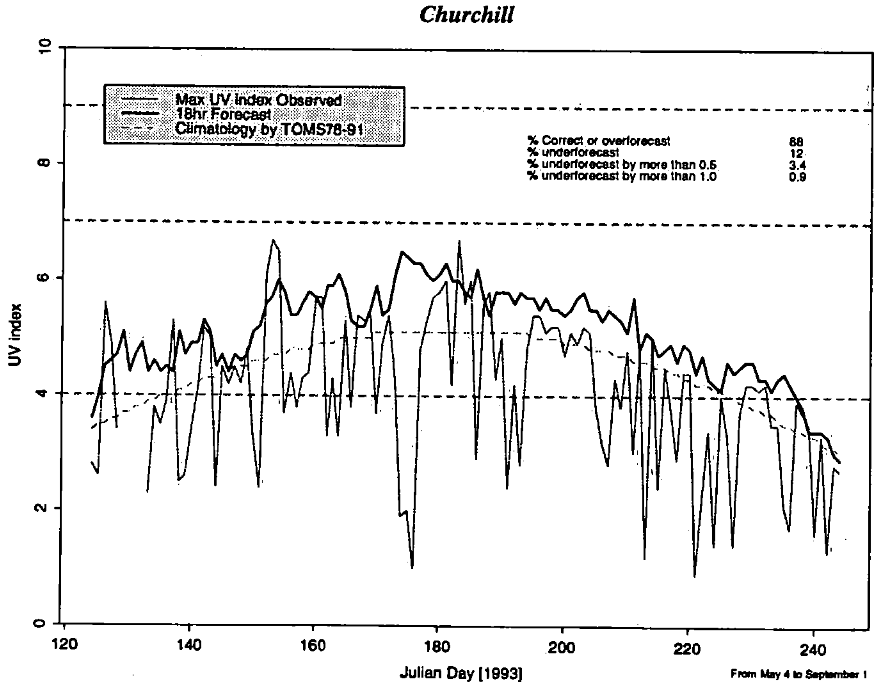

Figure 3.11: Timeseries of UV index.

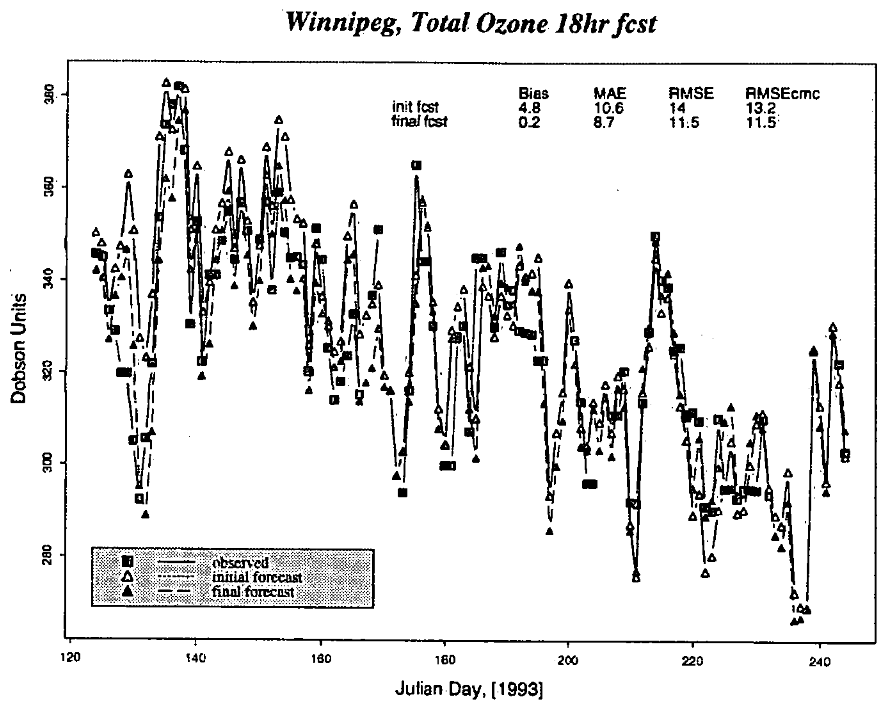

Figure 3.12: Timeseries of total ozone.

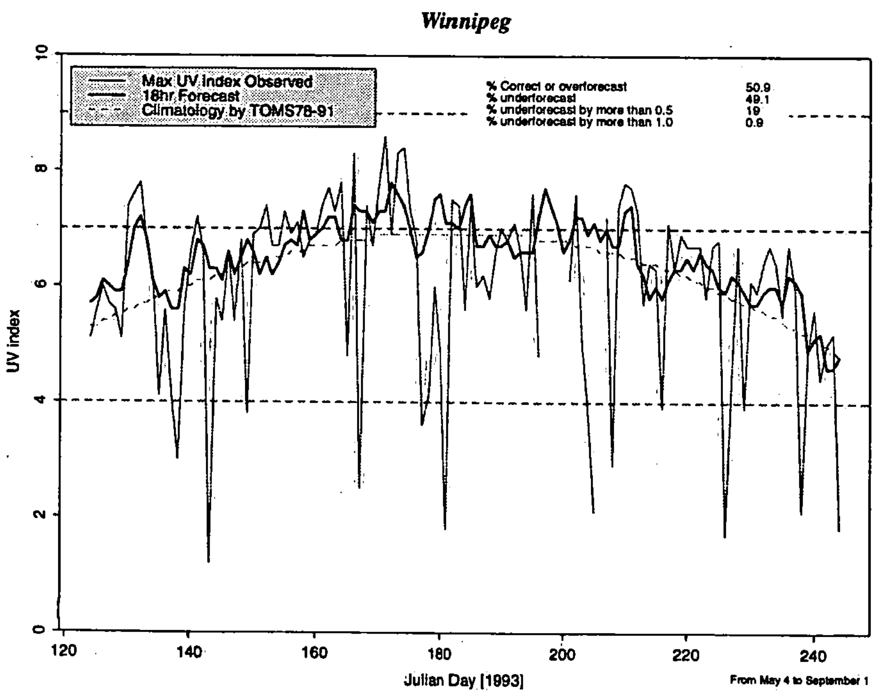

Figure 3.13: Timeseries of UV index.

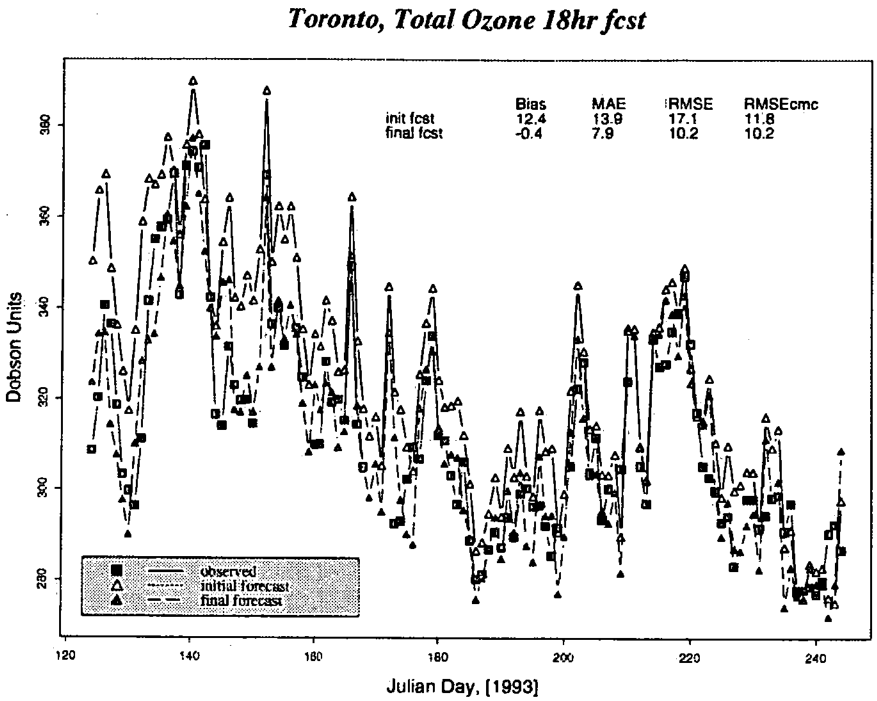

Figure 3.14: Timeseries of total ozone.

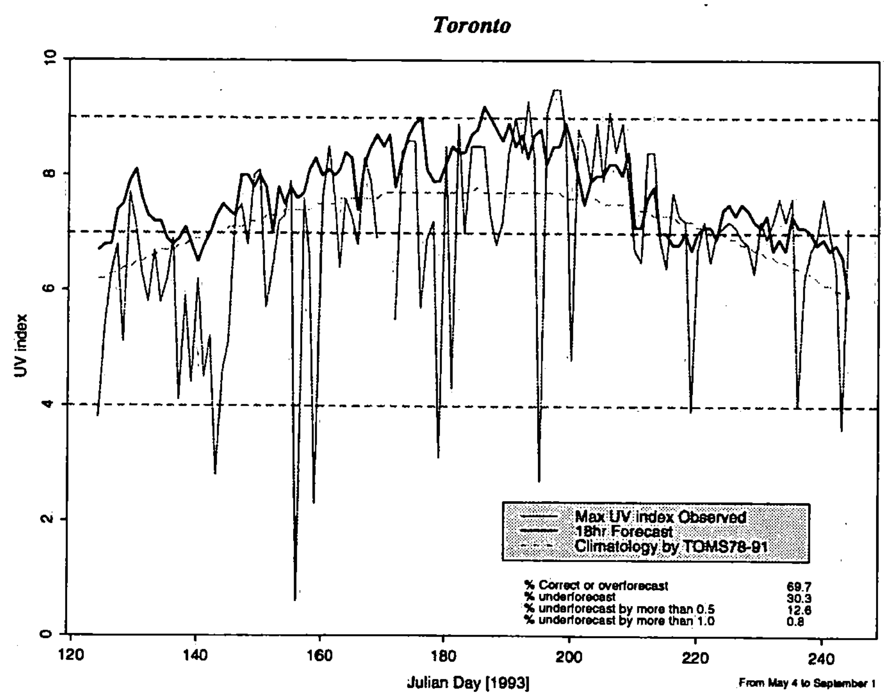

Figure 3.15: Timeseries of UV index.

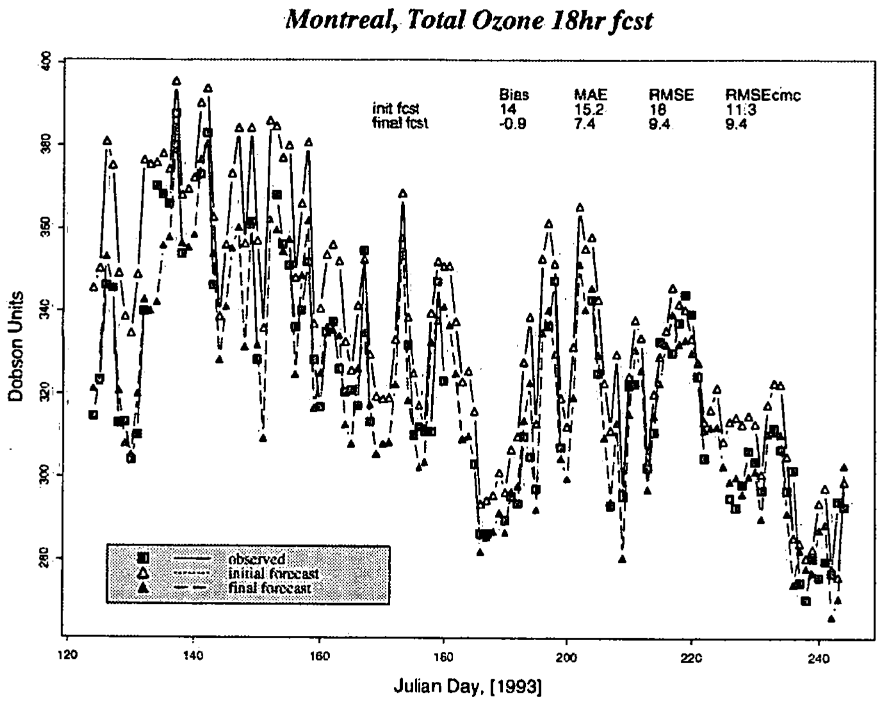

Figure 3.16 Timeseries of total ozone.

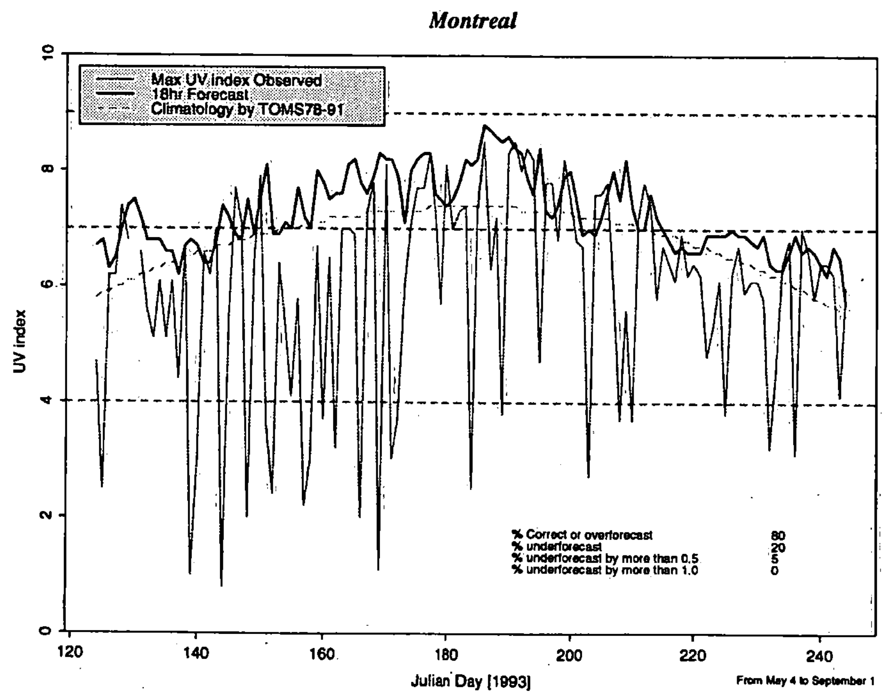

Figure 3.17: Timeseries of UV index.

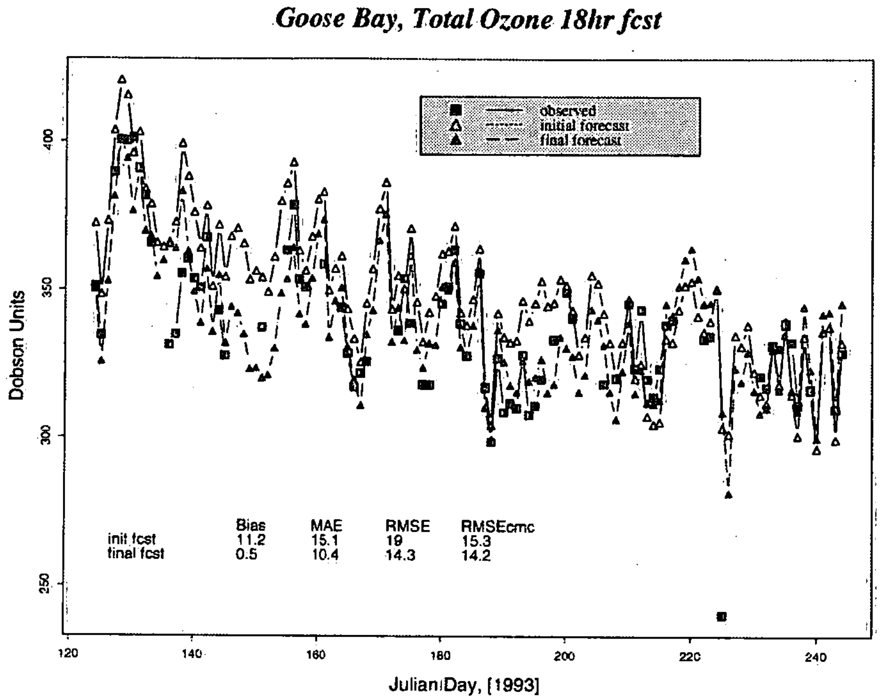

Figure 3.18: Timeseries of total ozone.

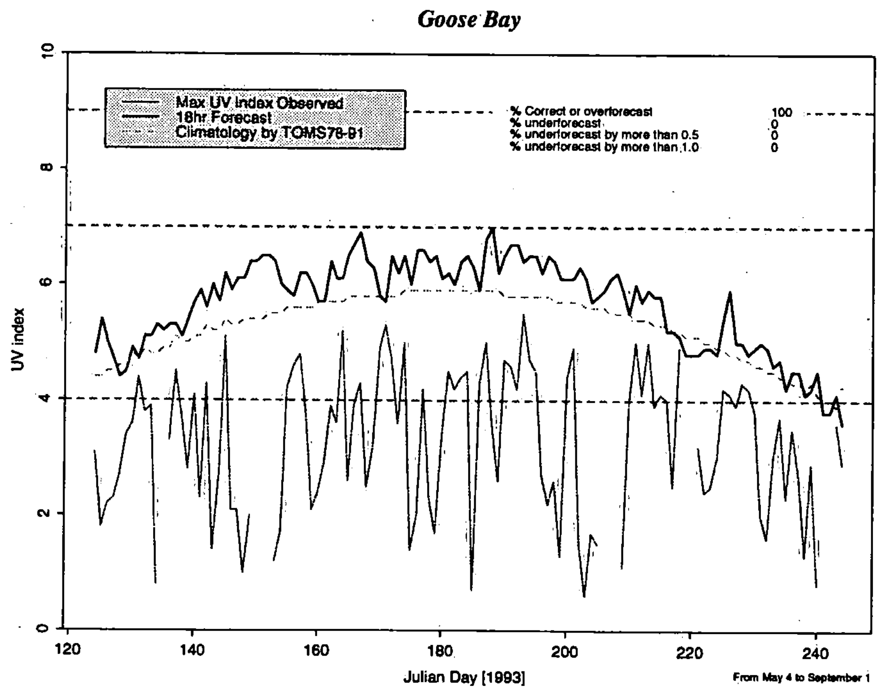

Figure 3.19: Timeseries of UV index.

Halifax, Total Ozone 18hr fcst

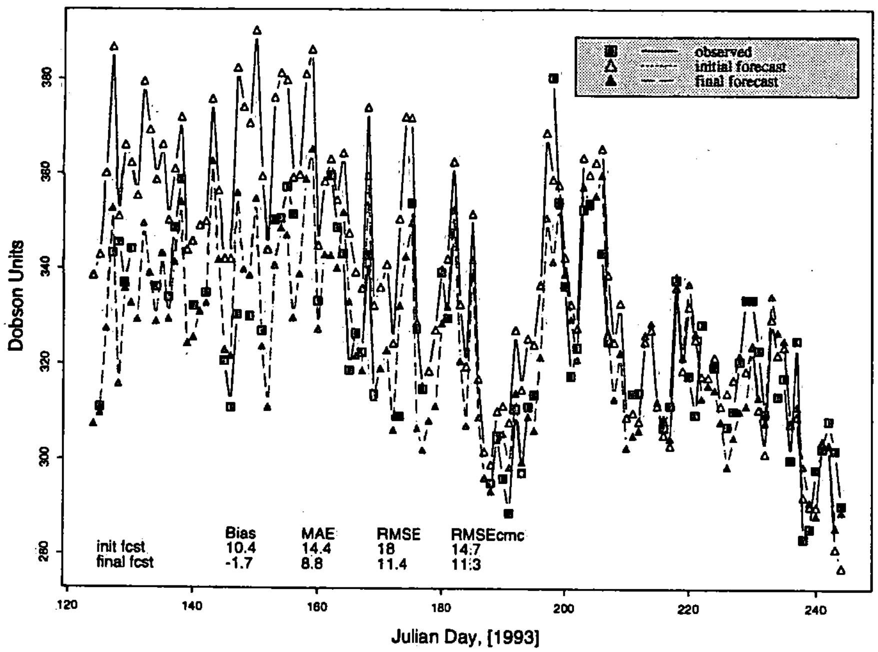

Figure 3.20: Timeseries of total ozone.

Halifax

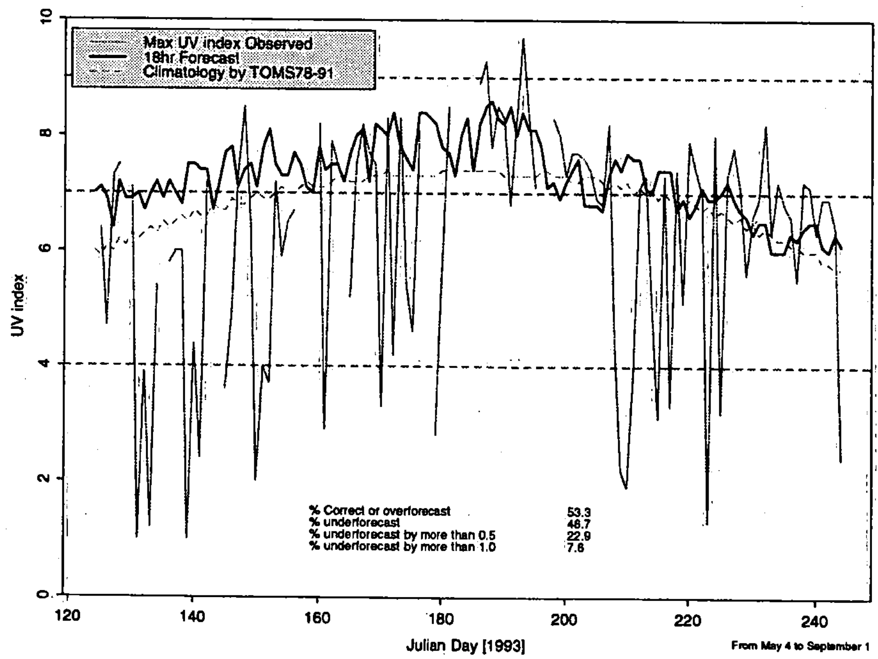

Figure 3.21: Timeseries of UV index.

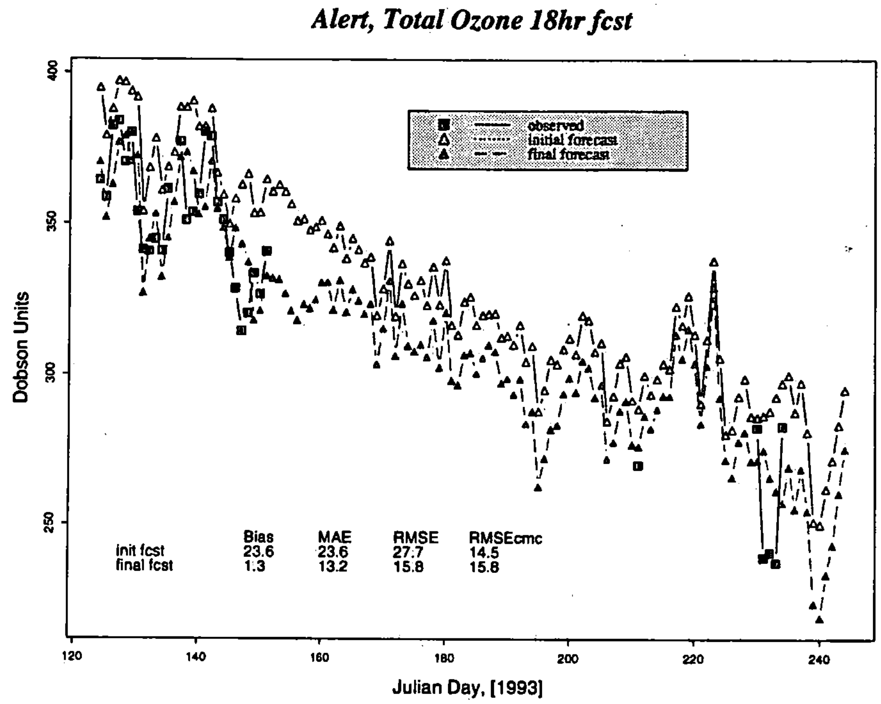

Figure 3.22: Timeseries of total ozone.

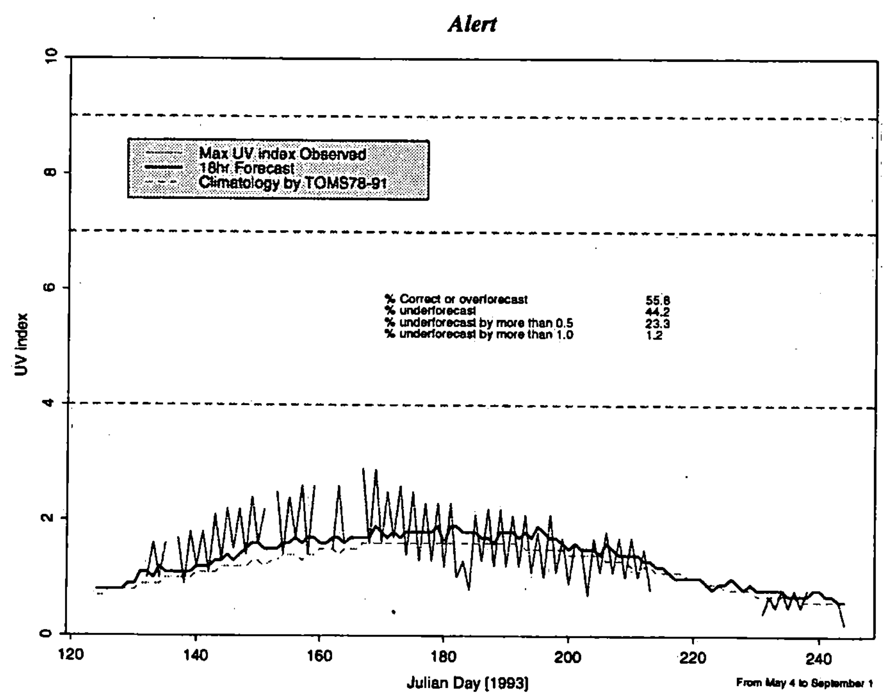

Figure 3.23: Timeseries of UV index.

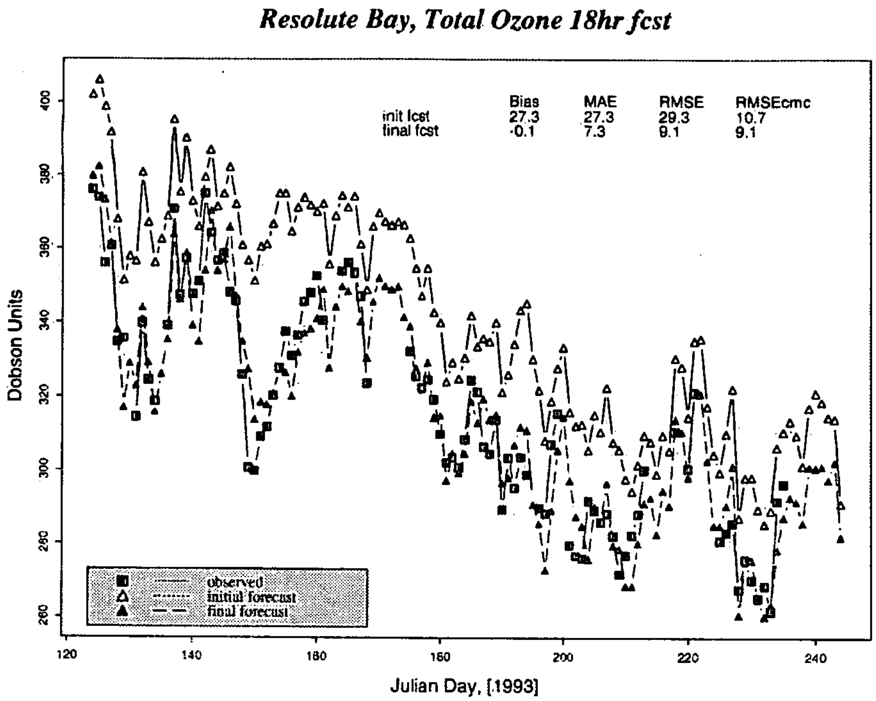

Figure 3.24: Timeseries of total ozone.

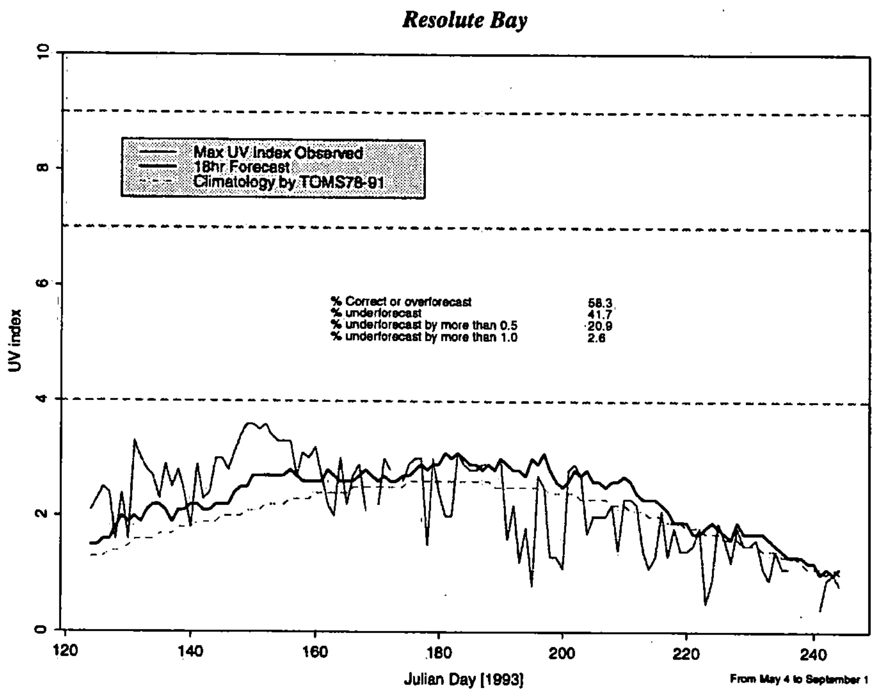

Figure 3.25: Timeseries of UV index.

on the graph as "% underforecast". The "%correct or overforecast" not only includes clear-sky cases which were genuinely overforecast, but also includes cases where the observed value has been reduced by cloud effects. The graphs also include a trace of the climatological clear sky UV values, obtained from the ozone climatology (Burrows et al, 1993). The UV graphs show that typically 50 to 60% of the UV forecasts are correct or underforecast, and that less than 3% are underforecast by an index value of more than 1.0.

Figure 3.26 shows more overall results, a timeseries of ozone forecasts and observations over all stations and figure 3.27, a pie chart of percentage correct or overforecast UV index values for all stations. The ozone timeseries plot must be carefully interpreted. Since different stations report ozone on different days, some of the day-to-day variation in the points on the graph is due to variations in the station sets that were used to compute averages on each day. Therefore, both forecast and observed timeseries were smoothed by

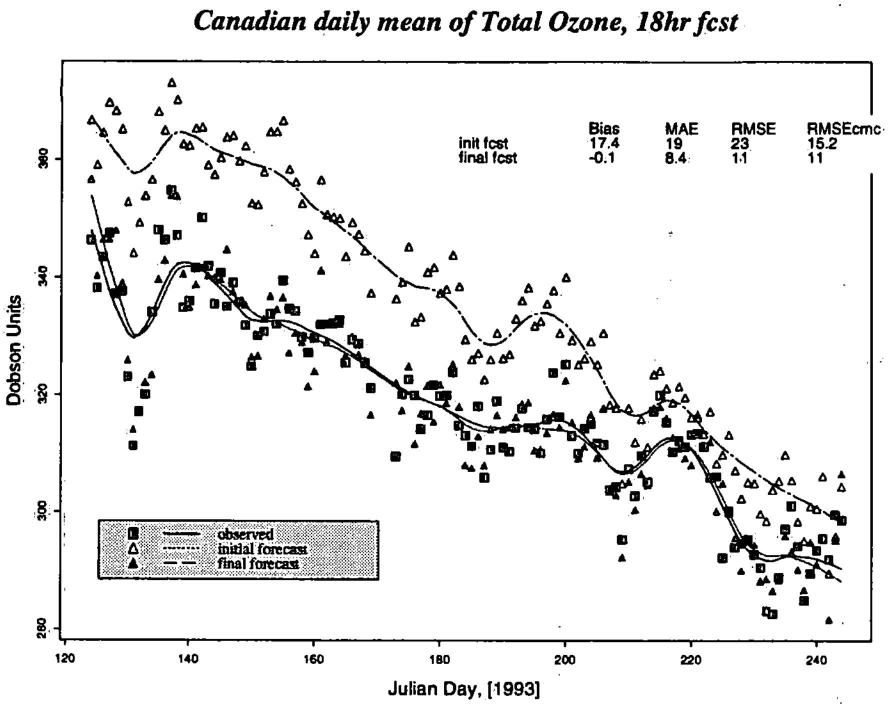

Figure 3.26: Average of total ozone in Canada for the 18hr forecast.

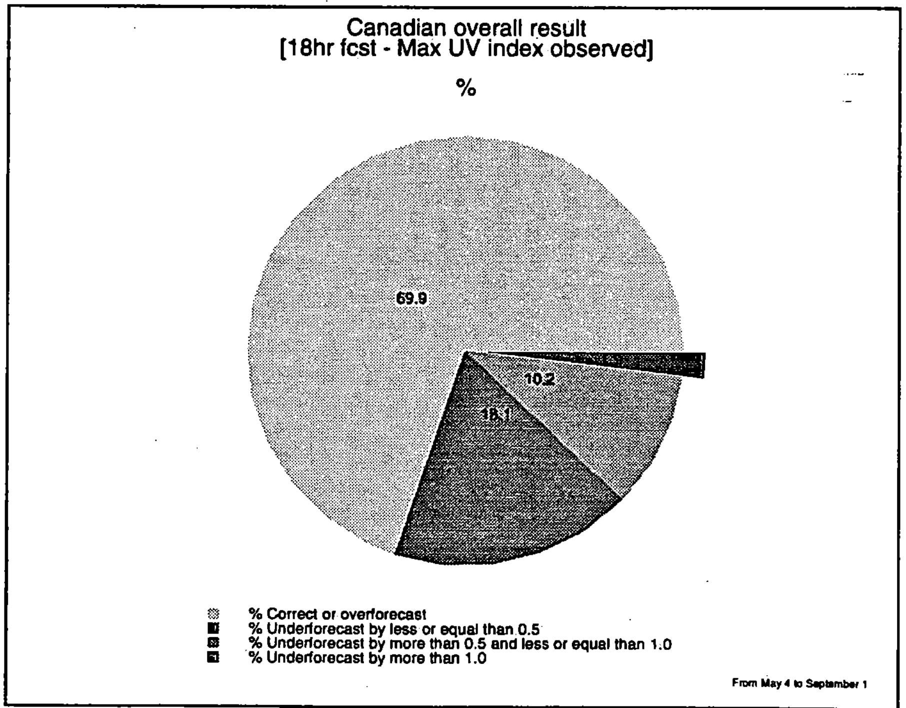

Figure 3.27: Skill of the UV index forecast in Canada.

means of a local regression smoother. Points were included only when three or more observations were available on a given day. Daily averages for both forecast and observations were computed using only the stations for which an observation was available on each day.

The information on figure 3.26 clearly shows the main overall features of the results and serves to summarize them: First, the bias in the initial forecasts is positive throughout (overforecasting) and decreases in magnitude after the middle of the summer. This, as stated above is due to the abnormally low observed ozone thickness early in 1993, which could not be explained by the meteorological variables. Second, the correction procedure reliably removes the bias. Third, the RMSE corrected for bias is lowered about 4 DU, by the correction procedure from 15 to 11. Once again, due consideration must be given to the fact that the verification was carried out only for Canadian locations equipped with Brewer spectrophotometers, and that the correction procedure was applied using the same dataset that was used in the verification.

Figure 3.27 shows that 30% of the forecast UV index values were too low when compared with the maximum daily values observed by the Brewer instruments. Less than 2% were underforecast by more than 1 unit of the UV index.

3.3 Case study for Toronto, June 1, 1993

Figure 3.28 shows the 18:00 UTC surface map (without isobars) for the Canadian area. The observed daily total ozone values for that day are plotted on the map. The main features are the ridge of high pressure from Newfoundland to the Northwest Territories, the cold front just southeast of the lower lakes, and the low over James Bay. Figure 3.29 is the corresponding (6 hours earlier) 250 hPa analysis, showing also an upper ridge from the Northwest Territories through Labrador and an elongated low northwest to southeast across northern Manitoba and Ontario. The two cyclonic vorticity centers associated with the low are clearly seen from the cloud structure on the satellite picture (Figure 3.30) and are marked with an "X".

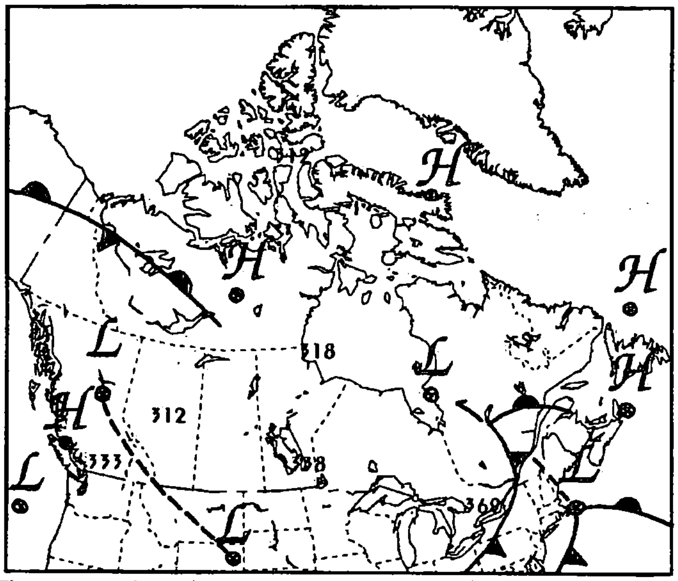

Figure 3.28: Synoptic situation over Canada on june 1, 1993 at 18:00 UTC. Data are the observed total ozone values in Dobson units.

Figure 3.31 is the 18h forecast of total ozone, valid for 18 UTC June 1. It is easily seen that the pattern corresponds quite well with the 250 hPa pattern, with ozone maxima in areas of cyclonic vorticity, for example the low over Ontario, and ozone minima in the higher pressure areas of the Northwest Territories. This would be expected since the 250 hPa height is the first predictor of the mid-latitude equation for summer, and reflects the tendency for ozone thickness to be higher in the vicinity of troughs and frontal zones where the tropopause is lower, and to be lower in ridges.

The following is a numerical example of the application of the correction procedure in this case. The forecast value for Toronto is 368.8 DU, interpolated from the initial forecast map (*DI*). For June 1, that initial forecast value would be about 0.3 of the regression value from the northern equation and 0.7 of the regression value from the midlatitude equations. The previous correction field value for Toronto was 26.7 DU, a value to be updated for use to make today's corrected forecast. The adjustment to the correction field (*DCFIELD*) is found as follows:

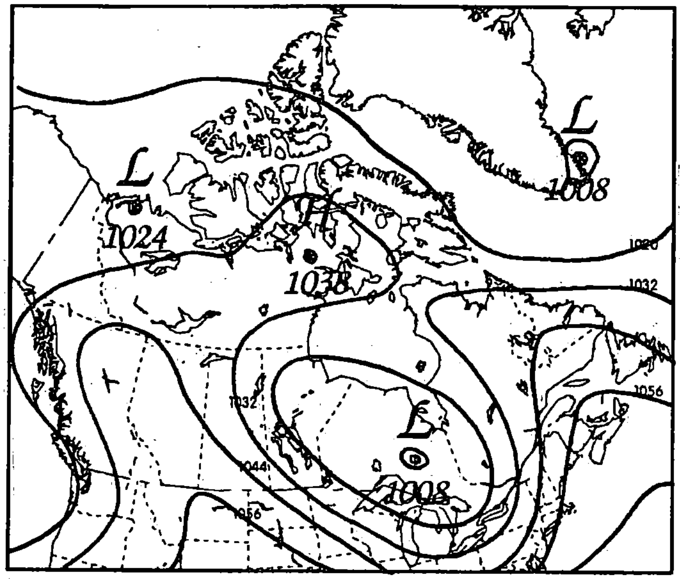

Figure 3.29: The 250 hPa surface pressure on june 1, 1993 at 12:00 UTC. Heights are in decameter.

No observation is available for Toronto today (cloudy on May 31). Thus a surrogate value of the residual must be found using yesterday's observation. The surrogate residual is computed from the actual residuals available at the other stations shown in table 3.2:

Table 3.2: Data used to calculate the residual in Toronto for the 18hr fcst valid on June 1, 1993.

STN	DU (300593 18Z) DU	OBS DU	RESIDUAL (DU - OBS) DU	$DIST_{YYZ-STN}$ KM
YXD	306.1	306.4	-0.3	2755
WLT	333.0	341.0	-8.0	4345
YRB	318.6	309.1	9.5	3520
YYR	320.4	337.2	-16.8	1755
YXE	325.4	332.8	-7.4	2209
YWG	362.9	357.0	5.9	1502
YHZ	323.8	327.0	-3.2	1260

The distances between Toronto and the stations where residuals are available today are also in table 3.2.

Yesterday (May 30), the residual at Toronto was 2.7 DU and today's *DCFIELD* was 1.62 DU. Then, these values can be substituted into equations 2.4 and 2.6 to give Toronto's surrogate residual, -3.8 DU. Then, from equations 2.7 and 2.8,

$$DU_{YYZ} = 338.8 - (26.7 + 0.6 * (-3.8)) = 364.4 \text{ DU}$$

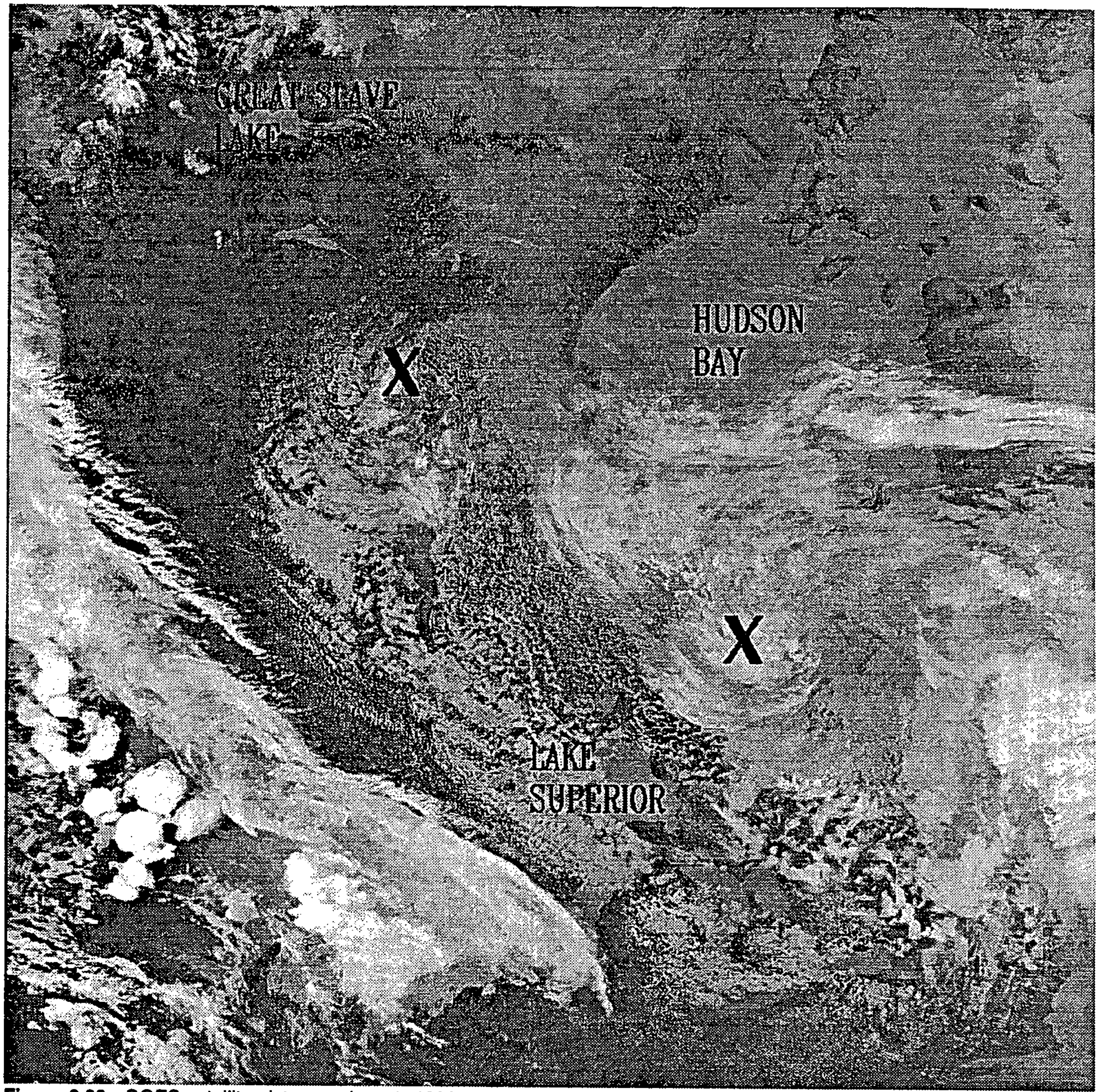

Figure 3.30: GOES satellite picture on june 1, 1993 over eastern Canada. "X" represent maximum vorticity.

Toronto's corrected forecast value is thus 364.4 DU. The verifying value on June 1 was 369.4 DU, only 5 DU from the final forecast value, but, only 0.6 DU from the initial forecast value. This is an example where the correction went in the wrong direction, making the forecast slightly worse.

The UV flux from equation 1.1 was 175.0 mWm^{-2}, which translates to a UV index of 7.0. The maximum UV index value reported on that day was 6.4.

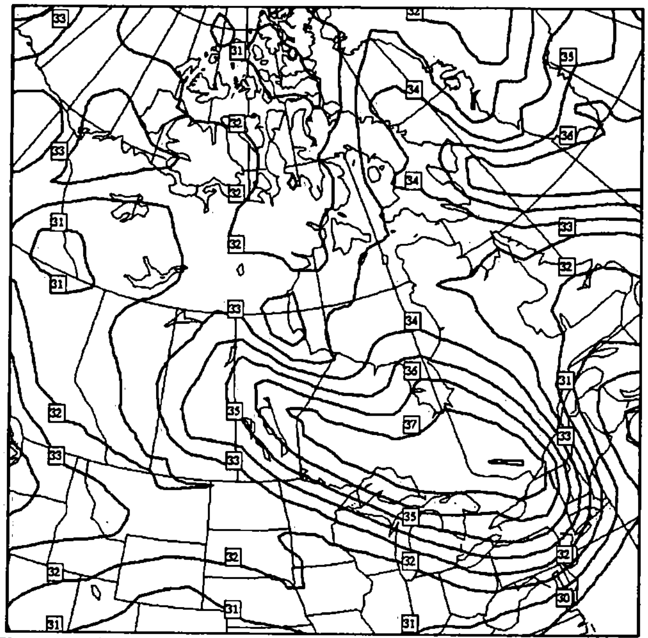

Figure 3.31: Total ozone forecast field on june 1, 1993 at 18:00 UTC. Values are in 10's of Dobson units.

Conclusion and Future Work

This report describes in some detail the Canadian ozone-UV forecast procedure that has been used in 1993 to forecast daily ozone and the UV index for Canada. Verification statistics are presented for the 1993 ozone and UV index forecasts, using observations from the 13 station Canadian network of Brewer spectrophotometers. The technique has been shown to improve substantially on the operational 1992 procedure and produces overall average total ozone error levels of 15 DU before and 11 DU after a correction based on yesterday's data is applied. The verification results also support the conclusion that abnormally low observed ozone thicknesses during the early part of the summer of 1993 were not described by the meteorological predictors and led to abnormally high positive biases in the forecasts.

Verification of the UV index directly is more problematic because of the effects of clouds on the observations. In this first verification attempt, we elected to verify the clear sky UV index as an indication of the maximum recorded daily UV value. As it is the underforecast cases that are of greatest concern, we concentrated on these, combining all correct or overforecast cases into one group, since we cannot tell whether the overforecasting was a genuine error or simply due to a reduction in the observed UV value because of cloud. Direct verification of the UV index will become more feasible when objective estimates of the effects of cloud are available.

The verification of the technique has so far been limited to comparisons with Brewer observations in Canada. Forecasts are produced for all of the Northern Hemisphere, and the forecast equations, which are based on hemispheric TOMS data, are valid for all parts of the Northern Hemisphere between 10 N and 75 N. This is a significant limitation of the verification, because the use of Brewer data both in the correction and in the verification might lead to an overestimate of the true accuracy of the forecasts.

It is clear that the greatest potential improvement of the ozone forecast system can be achieved by the incorporation of satellite data, in several ways. First, satellite data provides a new source of verification information with horizontal coverage that is as complete as the coverage of the forecasts. Second, satellite data, if it can be obtained in near real time, can be used as a persistence predictor to incorporate information on the longer-term non-meteorological variations in ozone depth that are not presently accounted for in the statistical forecasts. Third, satellite data provides an opportunity to obtain an analysis of ozone depth on a real time basis, for use in initialization of the ozone field as input to dynamic forecasts of ozone and for use in correction of the forecasts. Ideally, such an analysis would incorporate all sources of ozone measurements that are available, which might include TOVS data, Brewer data (both national and international), TOMS data from the new US instrument, TOMS data from METEOR 3, SBUV data, and eventually, data from the GOME instrument aboard ERS-2.

However much we are able to improve the forecasts and analysis of total ozone, it is also clear from an examination of timeseries of UV observations that the most important single cause of variation in the daily UV index values is not due to ozone, but due to clouds; variations in total ozone produce a rather modest modulation of the UV index. Thus the single best opportunity for improvements in the forecasts will be by attempting to produce an objective estimate of the variations in UV flux at the ground due to cloudiness variations. These can then be combined directly with the clear-sky UV values as now forecast. Work on this problem has started.

Date Due

OCT 20 2016			

Three Dark Figures
Making the Weather
In Folk, in Myth, in Legend,
A threefold test.
Shiva, Vishnu, Brahmin.
Father, Son, Holy Ghost.
Body, Mind, Spirit.
Triune, Triumvirate, Tribunal.
One is Isolate
Two is divisive
Three is Peace.
Three is Torment.
Three is Potent.
Power, Power, Power.
Air, Fire, Water.
Three Dark Figures,
Making the Weather.

Ron Baird, Sculptor